

Vortices in Atomic Bose-Einstein Condensates: an Introduction

Sankalpa Ghosh

Physics Department, Technion I.I.T. Haifa-32000, Israel

(Dated: November 12, 2018)

Abstract

The occurrence of vortices in atomic Bose-Einstein condensates (BEC) enables a description of their superfluid behaviour. In this article we present a pedagogical introduction to the vortex physics in trapped atomic BECs. The mechanism of the vortex nucleation in an atomic BEC is discussed in detail. We also discuss a recently proposed approach which treats the problem of vortex nucleation using a one-particle Schrödinger equation with non-local and chiral boundary conditions.

PACS numbers: 03.75.Kk, 03.75.Lm, 05.30.Jp, 67.40.Db

Contents

I. Introduction	3
II. Single-boson problem	6
A. Anisotropic case	7
B. Spherical oscillator (SO)	7
C. Two-dimensional isotropic harmonic oscillator (2DIO)	8
D. Characteristic frequency of vortex nucleation	9
III. Bogoliubov Description of a weakly interacting Bose gas	10
A. Classical approximation: Gross-Pitaevskii equation	12
B. Healing length of the condensate	13
C. Vortex solution of the GP equation – Quantization of circulation	13
D. Leading order corrections: Bogoliubov equations	14
E. Bogoliubov theory in a rotating frame	15
F. Characteristic frequency of vortex nucleation	16
IV. Gross-Pitaevskii equation and its linear stability analysis	19
A. Linear response analysis of the Gross-Pitaevskii equation	20
B. Condensate in a box	21
C. Thermodynamic instability of a vortex solution	22
V. Approximation schemes to study the behaviour of the condensate	25
A. The Thomas-Fermi approximation for an isotropic confinement	26
B. Non-isotropic traps	27
VI. Vortex solution in the Thomas-Fermi regime	28
A. Critical frequency of vortex nucleation in the TF approximation	29
VII. Hydrodynamic theory of the condensate	31
A. Time evolution of the condensate density and velocity	31
B. Classical hydrodynamic approximation	33
C. Collective excitations from the classical hydrodynamic theory	33
D. Hydrodynamic Modes for trapped condensates	34

E. Quadrupole modes in the presence of a vortex	37
VIII. Experiments on vortices in BEC	37
A. Rotating Bucket analogue for trapped atoms	39
B. Experimental realization of a rotating trap	39
C. How to detect a vortex?	40
D. Vortex nucleation in a deformed trap	41
E. Rotating the normal cloud	42
F. How good experiments agree with the theory?	42
IX. The Role of surface barrier in vortex nucleation	43
A. Landau criterion of superfluidity	44
B. The order-parameter at the surface of the cloud	45
C. Surface modes from the hydrodynamic theory	47
X. Role of boundary conditions in nucleating vortices	49
A. Chiral boundary conditions (CBC)	50
B. Spectrum with CBC and the vortex nucleation	52
C. Spectrum with CBC	52
D. Vortex nucleation at $\Omega > \Omega_{c1}$	55
XI. Vortex nucleation in a deformed trap	56
A. Stationary states in the rotating frame	56
B. Adiabatic switch on of the rotation	57
C. Sudden switch on of the rotation	58
XII. Conclusion and Outlook	60
References	60

I. INTRODUCTION

One of the prominent features of a superfluid is the way it behaves under rotation [1]. The second derivative of the free energy with respect to the rotational frequency is proportional to the superfluid density and vanishes for a normal fluid. Therefore a way to distinguish

between superfluids and normal fluids is through their response to rotation. In contrast to a normal fluid, which rotates like a rigid body at thermal equilibrium, the thermodynamically stable state of a superfluid does not rotate at low enough frequency. At higher frequencies the angular momentum appears as vortex filaments at which the superfluid density vanishes. The circulation of the velocity field flow around a closed contour which encircles the vortex, is quantized [2, 3]. This is a consequence of the properties of the macroscopic wavefunction, whose phase changes by an integer multiple of 2π around the vortex filaments. The atomic Bose-Einstein condensates (BEC) [4, 5, 6, 7] provide a system for which this superfluid behaviour can be studied in the weak-coupling regime.

In this article we present a detailed introduction to the problem of vortex nucleation in atomic Bose-Einstein condensates which includes the recent developments in this field following the experimental detection of vortices in BEC [8, 9, 10, 11, 12, 13, 14, 15, 16, 17]. Part of the contents overlaps with those of a recent review by Fetter and Svidzinsky[18] which is a much more broad based account of vortices in BEC in general. However we emphasized here the problem of vortex nucleation and provide also a detailed background theoretical framework aiming a more general readership.

The article is organized as follows In the first few sections we described in detail the vortices in trapped atomic condensates, the associated quantization of circulation, the thermodynamic stability of a vortex and the evaluation of the characteristic nucleation frequency of a vortex based on thermodynamic arguments. In Section II, we focus on a single boson problem in a harmonic confinement which has been detailed in a number of references (for example see chapter 6, ref. [19]). We discuss the results in a static as well as in a rotating reference frame. The rotating trap problem is important in view of the fact that the experiments on vortices in atomic condensates are generally performed in a rotating trap. We show why a vortex cannot be nucleated in a mechanically stable rotating harmonic trap if the bosons are non-interacting whereas a finite amount of interaction makes vortex states energetically feasible. In Section III, we describe the Bogoliubov theory which deals with weakly interacting bosons at very low temperature [20] (see [21] for a review and further developments). The extension of this theory to the trapped atomic condensate has been studied in a number of references [22, 23, 24, 25, 26, 27, 28, 29, 30, 31, 32] which includes the cases of static as well as the rotating traps and has been reviewed in [6, 7, 18]. We show how the Bogoliubov theory leads to the Gross-Pitaevskii (GP) equation [33, 34] which

is very successful in explaining the properties of the condensate at very low temperature as observed in recent experiments, both with and without vortices. We also discuss the meaning of the condensate wavefunction [35, 36] and how it is related to superfluidity (see chapter 5 of [37]). We then explain how the vortex solutions of the GP equation lead to the quantization of circulation, an idea which dates back to L. Onsager and R. P. Feynman [2, 3, 38].

This is followed by a discussion showing how the characteristic frequency of vortex nucleation in a trapped condensate can be found from the solution of the GP equation [39, 40, 41, 42, 43]. The main aspect of the Bogoliubov theory is the description of the weakly interacting bosons in terms of a condensate wavefunction and of non-interacting quasiparticles known as the Bogoliubov excitations. We discuss these Bogoliubov excitations and show how they determine the stability of a solution of the Gross-Pitaevskii equations. We emphasize the instability of a vortex solution in a static trap [24, 25, 31, 44] and clarify how this instability is removed when the trap is put into rotation [30, 44, 45]. We stress that this aspect explains why vortices are not thermodynamically stable below a characteristic rotational frequency of the trap [18, 45].

In Section V, we describe the Thomas-Fermi (TF) approximation [40, 41] which gives analytical expressions for experimentally measurable quantities while has been very successful in explaining the behaviour of a large condensate. We also discuss the correction to the TF approximation required to describe the condensate profile at the boundary. We describe the condensate profile with and without vortex under this approximation and mention how an analytic expression for the vortex nucleation can be derived under this approximation [46, 47, 48]. We then turn to the study of the collective excitations of the condensate within the TF approximation [27, 47]. For this we introduce the hydrodynamic description of the condensate and show how it leads to the dispersion law of the collective excitations [49]. We discuss in more detail the quadrupole mode [50] since it plays an important role in the process of vortex nucleation.

In section VIII, we discuss experiments experiments [8, 9, 10, 11, 12, 13, 14, 15, 16, 17] and compare them with the theoretical predictions. We mention how the experimental observations point out the limitation of the thermodynamic critical frequency of vortex nucleation and points towards a more local theory of vortex nucleation which we discuss in the next few sections. Vortices are nucleated from the surface. So to construct such

a local theory one needs to know the condensate profile and its collective excitations at the surface of the trap. To that purpose we first account for the correction to the TF approximation required to describe the condensate profile at the boundary [42, 51, 52]. Then we discuss how this correction is included into the hydrodynamic theory to find out the modified dispersion relation of the surface modes [53, 54, 55]. Once the dispersion relation of the surface modes are identified using the Landau criterion [56], it is possible to determine the rotational frequency for which a given surface excitation becomes unstable towards the vortex nucleation [32, 54, 55]. We particularly emphasize that the characteristic frequency determined in this way [55] agrees very well with the value experimentally observed [15].

In section X, we discuss a different approach we have proposed [57] to study the problem of vortex nucleation where one replaces the non-linear interaction term in the GP equation by a set of non-local and chiral boundary conditions. The problem we study is strictly two-dimensional. Such boundary conditions give a natural splitting of the Hilbert space of the problem into bulk and edge states (which are two-dimensional analogues of the surface states). We show that the characteristic frequency of the vortex nucleation determined in this way is very close to the values experimentally observed [15]. In experiments a rotated trap is deformed in the plane of the rotation [13]. If the deformation in the trap is not very large, it can be associated with a quadrupolar density deformation and the corresponding velocity field. The dynamics of this quadrupolar mode in the rotating frame determines the vortex nucleation in the condensate by overcoming a surface barrier. This issue has been investigated in detail both experimentally [13, 14, 17] as well as theoretically [58, 59, 60] which we also discuss briefly. We conclude our article by summarizing these discussions.

II. SINGLE-BOSON PROBLEM

We start our discussion by listing the results from the solutions of the time-independent Schrödinger equation of a trapped boson [19]), namely,

$$H_0\Phi(\mathbf{r}) = \left(-\frac{\hbar^2}{2m} + V_{tr}(\mathbf{r})\right)\Phi(x, y, z) = E\Phi(x, y, z) \quad (2.1)$$

The trap can be either static or rotating. In the later case the hamiltonian in the lab-frame is time-dependent. A time-independent hamiltonian (H_{rot}) is obtained by going into the co-rotating frame of the trap which is related to the static hamiltonian in the lab frame

(H_0) by

$$H_{rot} = H_0 - \boldsymbol{\Omega} \cdot \mathbf{L} \quad (2.2)$$

A. Anisotropic case

If the trap is harmonic the Schrödinger equation (2.1) rewrites

$$\left[-\frac{\hbar^2}{2m} \nabla^2 + \frac{m}{2} (\omega_x^2 x^2 + \omega_y^2 y^2 + \omega_z^2 z^2) \right] \Phi(x, y, z) = E \Phi(x, y, z) \quad (2.3)$$

The most general case is one in which all the trap frequencies are different. The problem is separable in Cartesian coordinates, namely, $\Phi(x, y, z) = \phi_1(x)\phi_2(y)\phi_3(z)$. The eigenfunctions and the energy eigenvalues are respectively those of a three dimensional harmonic oscillator and are defined by a set of three quantum numbers $\mathbf{n} = \{n_x, n_y, n_z\}$.

$$\Phi_{\mathbf{n}} = \pi^{3/2} 2^{-\frac{1}{2}(\sum_{\alpha} n_{\alpha})} e^{-\frac{1}{2}(\sum_{\alpha} b_{\alpha} x^2)} \prod_{\alpha} \sqrt{\frac{b_{\alpha}}{n_{\alpha}!}} H_{n_{\alpha}}(\alpha \sqrt{b_{\alpha}}) \quad (2.4)$$

$$E_{\mathbf{n}} = \sum_{\alpha} \left(n_{\alpha} + \frac{1}{2} \right) \hbar \omega_{\alpha} \quad (2.5)$$

Here $\alpha = x, y, z$. $H_n(\alpha \sqrt{b_{\alpha}})$ is a Hermite polynomial of degree n and

$$\sqrt{b_{\alpha}} = \sqrt{\frac{m\omega_{\alpha}}{\hbar}} = \frac{1}{a_{\alpha}} \quad (2.6)$$

where a_{α} is the harmonic oscillator length scale corresponding to the axis α . In this most general case of three distinct trap frequencies, the eigenfunctions and energy levels of the hamiltonian H_{rot} are not simply related to those corresponding to the non-rotating case. We shall not discuss this case any further. Rather in the following discussion we consider only some special cases of interest where such a simple relation exists.

B. Spherical oscillator (SO)

The hamiltonian is that of an isotropic or spherical oscillator with $\omega_x = \omega_y = \omega_z = \omega$. The problem is separable in spherical co-ordinates (r, θ, ϕ) . There

$$H_0 = \frac{\hbar^2}{2m} \left(-\frac{1}{r} \frac{d^2}{dr^2} r + \frac{\mathbf{L}^2}{r^2} + \frac{1}{2} m \omega^2 r^2 \right), \quad (2.7)$$

The eigenfunctions and eigenvalues are described by a set of three quantum numbers $\mathbf{n} = (n_r, l, l_z)$ where $n_r \in \mathbf{N}$; $l \in \mathbf{N}$; $-l \leq l_z \leq l$. The eigenfunctions are written as a product of a Laguerre polynomial (radial part) and of a Spherical harmonic (angular part).

$$\Phi_{\mathbf{n}} = b_{\omega}^{3/4} \frac{1}{\pi^{1/4}} (\sqrt{b_{\omega}} r)^l e^{-(\frac{r}{b_{\omega}})^2/2} \sqrt{\frac{2^{n_r+l+2} n_r!}{(2n_r + 2l + 1)!!}} L_{n_r}^{l+1/2}(b_{\omega} r^2) Y_{l,l_z}(\theta, \phi) \quad (2.8)$$

$$E_{\mathbf{n}} = \hbar\omega(2n_r + l + \frac{3}{2}) \quad (2.9)$$

where L_n^l is a Laguerre polynomial and Y_{l,l_z} is a spherical harmonic. These are simultaneous eigenfunctions of the hamiltonian and one of the three angular momentum operators. Conventionally, this component is identified with the z -axis namely

$$L_z \Phi_{\mathbf{n}} = l_z \Phi_{\mathbf{n}} \quad (2.10)$$

The energy is degenerate in l_z . If the spherical trap is rotated about the z -axis, with a rotational frequency Ω

$$H_{rot} = H_0 - \Omega L_z \quad (2.11)$$

The eigenfunctions of H_{rot} are identical to those defined in (2.8) but with the eigenvalues

$$E_{\mathbf{n}}^{rot}(\Omega) = \hbar\omega(2n_r + l(1 - \frac{l_z\Omega}{l\omega}) + \frac{3}{2}) \quad (2.12)$$

The l_z degeneracy is therefore lifted by the rotation.

C. Two-dimensional isotropic harmonic oscillator (2DIO)

Another case of interest corresponds to $\omega_x = \omega_y = \omega_{\perp} \neq \omega_z$. This trap geometry is particularly adopted in most of the experiments on atomic BEC. Using cylindrical polar co-ordinates (r, θ, z) one finds that the problem separates into a pair of harmonic oscillators namely an isotropic oscillator in the x - y plane and another one dimensional oscillator along the z -axis. The eigenfunctions can be written as a product of the eigenfunctions of a two-dimensional isotropic oscillator and of a one dimensional harmonic oscillator. The energy-eigenvalues are the sum of the corresponding eigenvalues. We also define the aspect ratio λ_R which gives the relative strength of the confinement of the one dimensional harmonic oscillator in the z -direction to the confinement of the isotropic oscillator, namely,

$$\lambda_R = \frac{\omega_z}{\omega_{\perp}} \quad (2.13)$$

Since this pair of oscillators with different dimensionalities are decoupled from each other we shall consider only the motion of the isotropic harmonic oscillator. In (r, θ) co-ordinates the hamiltonian writes as

$$H_{\perp} = -\frac{\hbar^2}{2m} \left[\frac{\partial}{\partial r} \left(r \frac{\partial}{\partial r} \right) + \frac{L_z^2}{r^2} \right] + \frac{1}{2} m \omega_{\perp}^2 r^2 \quad (2.14)$$

The eigenfunctions and energy eigenvalues can be written in terms of two quantum numbers $\{\mathbf{n}_{\perp}\} = (n, l_z)$

$$\Phi_{\mathbf{n}_{\perp}} = \left(\frac{b_{\omega_{\perp}}^{l_z+1}}{\pi} \frac{n!(n+l_z)!}{n!^2 l_z!^2} \right)^{1/2} r^{|l_z|} e^{il_z \theta} e^{-\frac{b_{\omega_{\perp}} r^2}{2}} {}_1F_1(-n, |l_z|+1; b_{\omega_{\perp}} r^2) \quad (2.15)$$

$$E_{\mathbf{n}_{\perp}} = (2n + |l_z| + 1) \hbar \omega_{\perp} \quad (2.16)$$

where $b_{\omega_{\perp}} = \frac{m \omega_{\perp}}{\hbar}$, $n \in \mathbf{N}$, $l_z \in \mathbf{Z}$ and ${}_1F_1(\alpha', \beta'; x)$ is a confluent hypergeometric function. Those are eigenstates of the angular momentum operator L_z with eigenvalues l_z . If the trap is rotated about the z -axis, the corresponding hamiltonian is given by

$$H_{rot} = H_{\perp} - \Omega L_z \quad (2.17)$$

whose eigenfunctions are identical to those in (2.15) with the eigenvalues

$$E_{n,l_z}^{rot} = (2n + |l_z| - \frac{\Omega}{\omega_{\perp}} l_z + 1) \hbar \omega_{\perp} \quad (2.18)$$

We shall use latter the equivalent expression of the hamiltonian in the rotating frame

$$H_{rot} = \frac{1}{2m} (\mathbf{p} - m \mathbf{A}_{\Omega})^2 + \frac{1}{2} m (\omega_{\perp}^2 - \Omega^2) r^2 \quad (2.19)$$

where $\mathbf{A}_{\Omega} = \boldsymbol{\Omega} \times \mathbf{r}$ and $\boldsymbol{\Omega} = (0, 0, \Omega)$. This is the Landau hamiltonian of a particle in a transverse magnetic field $\mathbf{B}_{\Omega} = 2\boldsymbol{\Omega}$ (written in the symmetric gauge) and in a parabolic confinement $\frac{1}{2} m (\omega_{\perp}^2 - \Omega^2) r^2$.

D. Characteristic frequency of vortex nucleation

For a spherical oscillator, with $\Omega < \omega$, the ground state is $(n, l, l_z) = (1, 0, 0)$ always remains the ground state. Similarly the ground state of the isotropic oscillator such that $\Omega < \omega_{\perp}$ is $(n, l_z) = (0, 0)$. For a set of non-interacting rotating trapped bosons, a vortex

is nucleated if in the co-rotating frame a state with higher angular momentum quantum number becomes the ground state of the system. If this happens the corresponding rotational frequency is the characteristic nucleation frequency of the first vortex (Ω_{c1}). According to this definition, in either cases of SO and 2DIO, the the first vortex ($l_z = 1$) is nucleated when the energy of the $l_z = 1$ state in the rotating frame is equal to the ground state energy ($l_z = 0$). Using (2.12) and (2.18) and the relation $E_{\mathbf{n}}^{rot} = E_{\mathbf{n}} - \Omega l_z$, we therefore get

$$\Omega_{c1} = \frac{N_0(E_{\mathbf{n}}(n_r = 1, l = 1, l_z = 1) - E_{\mathbf{n}}(n_r = 1, l = 0, l_z = 0))}{N_0\hbar} = \omega \quad (SO) \quad (2.20)$$

$$\Omega_{c1} = \frac{N_0(E_{\mathbf{n}}(n = 1, l_z = 1) - E_{\mathbf{n}}(n = 1, l_z = 0))}{N_0\hbar} = \omega_{\perp} \quad (2DIO) \quad (2.21)$$

For either $\Omega = \omega_{\perp}$ or $\Omega = \omega$, the confinement potential is compensated by the centrifugal force. The trapped condensate is therefore unstable at this point. Therefore, non-interacting bosons in a trap cannot have stable vortex solutions at $T = 0$. Since experimentally vortices are nucleated before this limit is reached and at very low temperatures ($k_B T \ll \hbar\omega$) one concludes that a finite amount of interactions among bosons leads to the vortex nucleation. Thus, in order to study vortex nucleation, one needs to include interaction between bosons. We shall first consider the limit of a weakly interacting gas within the framework of the Bogoliubov [20] theory. We shall assume repulsive and local interactions among the bosons. The next section is devoted to the description of the Bogoliubov theory.

III. BOGOLIUBOV DESCRIPTION OF A WEAKLY INTERACTING BOSE GAS

The Bogoliubov description of a weakly interacting Bose gas (with and without confining potential) has been detailed in a large number of references [4, 5, 6, 7, 19, 21, 22, 23, 61]. We start with the following interacting hamiltonian for a N -boson system

$$H_{mb} = \sum_{i=1}^N \left(-\frac{\hbar^2}{2m} \nabla_i^2 + V_{tr}(\mathbf{r}_i) \right) + g \sum_{i,j} \delta(\mathbf{r}_i - \mathbf{r}_j) \quad (3.1)$$

where $g = \frac{4\pi\hbar^2 a}{m}$, m is the mass of a boson, a is the s -wave scattering length which characterizes the repulsive delta-function interaction. Also

$$V_{tr} = \frac{1}{2}m(\omega_x^2 x^2 + \omega_y^2 y^2 + \omega_z^2 z^2) \quad (3.2)$$

In a second quantized form, the grand-canonical many-boson hamiltonian is

$$\hat{F} = \int d\mathbf{r} \hat{\psi}^\dagger(\mathbf{r}) \left(-\frac{\hbar^2}{2m} \nabla^2 + V_{tr}(\mathbf{r}) \right) \hat{\psi}(\mathbf{r}) + \frac{g}{2} \int d\mathbf{r} \hat{\psi}^\dagger(\mathbf{r}) \hat{\psi}^\dagger(\mathbf{r}) \hat{\psi}(\mathbf{r}) \hat{\psi}(\mathbf{r}) - \mu \hat{N} \quad (3.3)$$

where $\hat{N} = \int d\mathbf{r} \hat{\psi}^\dagger(\mathbf{r}) \hat{\psi}(\mathbf{r})$ is the number operator and μ is the chemical potential. The bosons field operators satisfy

$$[\hat{\psi}(\mathbf{r}), \hat{\psi}^\dagger(\mathbf{r}')] = \delta(\mathbf{r} - \mathbf{r}') ; \quad [\hat{\psi}(\mathbf{r}), \hat{\psi}(\mathbf{r}')] = [\hat{\psi}^\dagger(\mathbf{r}), \hat{\psi}^\dagger(\mathbf{r}')] = 0 \quad (3.4)$$

In general, the field operator $\hat{\psi}(\mathbf{r})$ can be expanded as

$$\hat{\psi}(\mathbf{r}) = \sum_{\mathbf{n}} \Phi_{\mathbf{n}}(\mathbf{r}) a_{\mathbf{n}} \quad (3.5)$$

where $\Phi_{\mathbf{n}}(\mathbf{r})$ are single-particle wavefunctions and $a_{\mathbf{n}}$ are the corresponding annihilation operators [61]. They obey the commutation rules:

$$[a_{\mathbf{n}_1}, a_{\mathbf{n}_2}^\dagger] = \delta_{\mathbf{n}_1, \mathbf{n}_2} , \quad [a_{\mathbf{n}_1}, a_{\mathbf{n}_2}] = 0 , \quad [a_{\mathbf{n}_1}^\dagger, a_{\mathbf{n}_2}^\dagger] = 0 . \quad (3.6)$$

Bose-Einstein condensation occurs when the number of atoms of a particular single-particle state becomes very large: $\equiv N_0 \gg 1$ and the ratio N_0/N remains finite in the thermodynamic limit $N \rightarrow \infty$. In the limit $N \rightarrow \infty$ the states with N_0 and $N_0 \pm 1$ atoms correspond to the same physical configuration. Thus the operators a_0 and a_0^\dagger can be considered as *c*-numbers since their commutator is negligible in comparison to N_0 . Therefore one sets $a_0 = a_0^\dagger = \sqrt{N_0}$. The above definition for the Bose-Einstein condensation holds for the non-interacting gas of bosons.

In presence of the interaction this definition of Bose-Einstein condensation in terms of the macroscopic occupation of a single boson eigenstate needs to be generalized. The generalization is done by requiring that one of the eigenvalues of the one body density matrix, namely the quantity $\langle \hat{\psi}^\dagger(\mathbf{r}) \hat{\psi}(\mathbf{r}) \rangle$ is macroscopic [62]. We shall not discuss this issue here and for details see chapter 1 of [5]. Thus the field operator $\hat{\psi}(\mathbf{r})$ can be written as a sum of a *c* number $\Psi(\mathbf{r}) = \sqrt{N_0} \Phi_0$, plus a correction $\delta\hat{\psi}(\mathbf{r})$,

$$\hat{\psi}(\mathbf{r}) = \Psi(\mathbf{r}) + \delta\hat{\psi}(\mathbf{r}) \quad (3.7)$$

Here Φ_0 is the macroscopically occupied single particle state. The classical field $\Psi(\mathbf{r})$ is defined as the condensate wavefunction. It is normalized by demanding

$$\int d\mathbf{r} |\Psi(\mathbf{r})|^2 = N_0 \quad (3.8)$$

such that N_0 is the total number of particles in the condensate. Plugging (3.7) in the expression for the free energy (3.3) and neglecting terms higher than quadratic in $\delta\hat{\psi}(\mathbf{r})$ and its adjoint finally yields,

$$\begin{aligned}\hat{F} = & \int d\mathbf{r} \Psi^* [H_0 - \mu + \frac{g}{2} |\Psi(\mathbf{r})|^2] \Psi(\mathbf{r}) \\ & + \int d\mathbf{r} \left(\Psi^* [H_0 - \mu + g|\Psi(\mathbf{r})|^2] \delta\hat{\psi}(\mathbf{r}) + \delta\hat{\psi}^\dagger(\mathbf{r}) [H_0 - \mu + g|\Psi(\mathbf{r})|^2] \Psi(\mathbf{r}) \right) \\ & + \frac{1}{2} \int d\mathbf{r} \begin{pmatrix} \mathcal{L} & g\Psi^2(\mathbf{r}) \\ \delta\hat{\psi}^\dagger(\mathbf{r}) & \delta\hat{\psi}(\mathbf{r}) \end{pmatrix} \begin{pmatrix} \delta\hat{\psi}(\mathbf{r}) \\ \delta\hat{\psi}^\dagger(\mathbf{r}) \end{pmatrix} \end{aligned} \quad (3.9)$$

where $\mathcal{L} = -\frac{\hbar^2}{2m}\nabla^2 + V_{tr} - \mu + 2g|\Psi(\mathbf{r})|^2$. For later use we shall denote the 2×2 matrix which appears in the above expression as \mathcal{H}_B (Bogoliubov hamiltonian).

A. Classical approximation: Gross-Pitaevskii equation

The first term in the expression (3.9) involves only the condensate wave function $\Psi(\mathbf{r})$ and its minimization gives the stationary Gross-Pitaevskii(GP) equation [33, 34]

$$[H_0 + g|\Psi(\mathbf{r})|^2]\Psi(\mathbf{r}) = \mu\Psi(\mathbf{r}) \quad (3.10)$$

This is also known as the non-linear Schrödinger equation. The time dependent GP equation (for example see chapter 7 [4]) is obtained by replacing the $\mu\Psi(\mathbf{r})$ by $i\hbar\frac{\partial\Psi(\mathbf{r},t)}{\partial t}$:

$$i\hbar\frac{\partial\Psi(\mathbf{r},t)}{\partial t} = [H_0 + g|\Psi(\mathbf{r})|^2]\Psi(\mathbf{r}) \quad (3.11)$$

The consistency between two equations requires that under stationary conditions $\Psi(\mathbf{r},t)$ must evolve in time as $e^{-i\frac{\mu}{\hbar}t}$. The Gross-Pitaevskii energy functional which can be minimized to give the GP equation (3.10) is given by

$$E_{GP} = \int d\mathbf{r} \left[\frac{\hbar^2}{2m} |\nabla\Psi(\mathbf{r})|^2 + V_{tr}(\mathbf{r}) |\Psi(\mathbf{r})|^2 + \frac{g}{2} |\Psi(\mathbf{r})|^4 \right] \quad (3.12)$$

and the associated Lagrangian is

$$L_{GP} = \int d\mathbf{r} \left[\frac{i\hbar}{2} \left(\Psi^* \frac{\partial\Psi}{\partial t} - \Psi \frac{\partial\Psi^*}{\partial t} \right) - E_{GP}(\Psi, \Psi^*) \right] \quad (3.13)$$

The quantity $\Psi(\mathbf{r})$ is called the condensate wavefunction since it represents the coherent motion of all the particles in a condensate. It is different from the first quantized many body

wavefunction of the N -boson system which is a function of the co-ordinates of N bosons and in principle can be obtained from the diagonalization of the hamiltonian of this N -boson system (3.1). This wavefunction contains all correlations present in the many boson system whereas the condensate wavefunction only represents the coherent motion of all condensed particles. We shall not discuss this issue any further which is detailed in a number of references, for example, (chapter 7 of [19], [35, 36] chapter 5 of [37]).

B. Healing length of the condensate

We shall now define the healing length of the condensate from the GP equation. For a condensate without any confinement potential, the healing length is defined as the length over which the wave function changes appreciably from its unperturbed value under some perturbation. It describes the size of the vortex core and the length over which the density grows from zero to its bulk value in the vicinity of a boundary [39]. Without confinement (3.10) rewrites

$$\left[-\frac{\hbar^2}{2m} \nabla^2 + g|\Psi(\mathbf{r})|^2 \right] \Psi(\mathbf{r}) = \mu \Psi(\mathbf{r}) \quad (3.14)$$

The minimum energy configuration corresponds to a uniform condensate density given by $|\Psi(\mathbf{r})|^2 = \rho_0 = \frac{\mu}{g}$ since the kinetic energy of such a configuration vanishes. If the density is locally perturbed, then far away from the perturbation it approaches this constant value $\rho_0 = \frac{\mu}{g}$ again. The wavefunction can therefore be written as $\Psi(\mathbf{r}) = \sqrt{\rho_0}\psi(\mathbf{r})$ such that $\psi \rightarrow 1$ when $r \rightarrow \infty$. The GP equation then becomes

$$\left[-\frac{\hbar^2}{2m\rho_0 g} \nabla^2 + |\psi(\mathbf{r})|^2 \right] \psi(\mathbf{r}) = \frac{\mu}{\rho_0 g} \psi(\mathbf{r}) \quad (3.15)$$

from which we see that the kinetic energy term is appreciable only if the wavefunction varies beyond the length scale defined by

$$\xi = \sqrt{\frac{\hbar^2}{2m\rho_0 g}} = \frac{1}{(8\pi\rho_0 a)^{\frac{1}{2}}} \quad (3.16)$$

ξ is called the healing length or the coherence length of the condensate.

C. Vortex solution of the GP equation – Quantization of circulation

The solutions of the GP equation (3.10) can generally be written as $\Psi(\mathbf{r}) = |\Psi(\mathbf{r})|e^{iS(\mathbf{r})}$ (*Madelung transformation*). The associated current can be defined (for details, see §VII)

as

$$\mathbf{j}(\mathbf{r}) = \frac{\hbar}{2im} [\Psi(\mathbf{r})^* \nabla \Psi(\mathbf{r}) - \Psi(\mathbf{r}) \nabla \Psi(\mathbf{r})^*] = |\Psi(\mathbf{r})|^2 \frac{\hbar}{m} \nabla S(\mathbf{r}) = \rho(\mathbf{r}) \frac{\hbar}{m} \nabla S(\mathbf{r}) \quad (3.17)$$

The condensate velocity $\mathbf{v}_s(\mathbf{r})$ is therefore $\frac{\mathbf{j}(\mathbf{r})}{\rho(\mathbf{r})}$ and it is proportional to the gradient of a scalar function. The flow of the condensate is therefore irrotational except at the points where the phase is singular, namely

$$\nabla \times \mathbf{v}_s = \frac{\hbar}{m} \nabla \times \nabla S(\mathbf{r}) = 0 \quad (3.18)$$

This implies that the condensate can be rotated only through the formation of vortices such that the condensate density vanishes at the vortex cores. To illustrate this point let us assume that the trap is a perfect cylinder such that the wavefunction Ψ is an eigenfunction of the operator L_z . In the cylindrical co-ordinate the phase of such an eigenfunction can generally be written as $S(z, r, \theta) = \kappa\theta$ such that the wavefunction is given by

$$\Psi(z, r, \theta) = \Psi(z, r) e^{i\kappa\theta} \quad (3.19)$$

The single-valuedness of the wavefunction requires κ to be an integer. This leads to

$$\oint_{\Gamma} \mathbf{v}_s \cdot d\mathbf{r} = \frac{\hbar}{m} \oint_{\Gamma} \nabla S(\mathbf{r}) \cdot d\mathbf{r} = \oint_{\Gamma} \left(\frac{\kappa\hbar}{mr} \hat{\theta} \right) \cdot (dr\hat{r} + rd\theta\hat{\theta}) = \frac{\kappa h}{m} \quad (3.20)$$

Therefore the circulation of the local velocity \mathbf{v}_s along any closed contour Γ which includes the point where the phase is singular is quantized in units of $\frac{h}{m}$ [2, 3].

D. Leading order corrections:Bogoliubov equations

Coming to the next order correction to the condensate wavefunction, one notes that the first integral in (3.9) is a *c*-number which we called E_g and the second integral vanishes identically if $\Psi(\mathbf{r})$ is a solution of the GP equation (3.10). Since the hamiltonian $(H - E_g)$ (3.9) is quadratic in $\delta\hat{\psi}^\dagger$ and $\delta\hat{\psi}$ it can be written in a diagonalized form, namely,

$$H - E_g = \sum_{\lambda} E_{\lambda} a_{\lambda}^\dagger a_{\lambda} \quad (3.21)$$

through the following Bogoliubov transformations

$$\delta\hat{\psi}(\mathbf{r}) = \sum_{\lambda} (u_{\lambda}(\mathbf{r}) a_{\lambda} + v_{\lambda}^*(\mathbf{r}) a_{\lambda}^\dagger) \quad (3.22)$$

such that u_λ and v_λ satisfies the following set of the eigenvalue equations

$$\begin{aligned}\mathcal{L}u_\lambda(\mathbf{r}) + g\Psi^2(\mathbf{r})v_\lambda(\mathbf{r}) &= E_\lambda u_\lambda(\mathbf{r}) \\ \mathcal{L}v_\lambda(\mathbf{r}) + g\Psi^{*2}(\mathbf{r})u_\lambda(\mathbf{r}) &= -E_\lambda v_\lambda(\mathbf{r})\end{aligned}\quad (3.23)$$

Unlike \mathcal{H}_B in (3.9) which (apart from the c-number E_g) defines a set of interacting bosons, the hamiltonian (3.21) describes non-interacting quasiparticles and the state of wavefunction $\Psi(\mathbf{r})$ which satisfies the GP equation is the corresponding vacuum. The wavefunction $\Psi(\mathbf{r})$ is characterized by its winding number κ and for each κ have its corresponding Bogoliubov quasiparticles. The quasiparticles are bosons and are related to the original bosons by the transformation (3.22). The commutators of $a_\lambda^\dagger, a_\lambda$ are same as those for the ordinary bosons (3.6). For more details see [7]. Since the energy of this quasiparticle is defined with respect to the condensate energy E_g , the presence of a Bogoliubov quasiparticle with negative energy and the normalization $\langle u_\lambda | u_\lambda \rangle - \langle v_\lambda | v_\lambda \rangle = +1$ implies an energetic instability for the solution of the GP equation. Such instability is known as the thermodynamic instability. Ψ being a solution of a non-linear equation there is also another kind of instability which is known as the dynamical instability. This instability determines whether there exists time-dependent fluctuations around Ψ whose amplitude exponentially grows over time and destabilizes it. Relation between these two types of (in)stabilities will be discussed in section §IV A.

E. Bogoliubov theory in a rotating frame

Stable vortex solutions are obtained in rotating trapped condensates which consist of bosonic atoms (atoms with integer spin). Therefore we mention the structure of the Bogoliubov theory in a rotating frame which has been studied in [30, 32]. In the rotating frame the second quantized grand-canonical hamiltonian (3.3) is

$$\hat{F}_{rot} = \hat{F} - \hat{\psi}^\dagger(\mathbf{r})(\boldsymbol{\Omega} \cdot \mathbf{L})\hat{\psi}(\mathbf{r})d\mathbf{r} \quad (3.24)$$

After the Bogoliubov decomposition we obtain

$$\hat{F}_{rot} = \hat{F} + \int d\mathbf{r} [\Psi^*(\mathbf{r})(\boldsymbol{\Omega} \cdot \mathbf{L})\Psi(\mathbf{r}) + \delta\hat{\psi}^\dagger(\mathbf{r})(\boldsymbol{\Omega} \cdot \mathbf{L})\Psi(\mathbf{r})] \quad (3.25)$$

$$+ [\Psi^*(\mathbf{r})(\boldsymbol{\Omega} \cdot \mathbf{L})\delta\hat{\psi}(\mathbf{r}) + \delta\hat{\psi}^\dagger(\mathbf{r})(\boldsymbol{\Omega} \cdot \mathbf{L})\delta\hat{\psi}(\mathbf{r})]. \quad (3.26)$$

where \hat{F} is given by (3.9). By keeping only the terms which involve only the condensate wavefunction, we obtain the GP equation in the rotating frame, namely

$$[H_0 + g|\Psi(\mathbf{r})|^2 - \boldsymbol{\Omega} \cdot \mathbf{L}] \Psi(\mathbf{r}) = \mu \Psi(\mathbf{r}) \quad (3.27)$$

The corresponding Bogoliubov hamiltonian in the rotating frame becomes

$$\mathcal{H}_B(\text{rot}) = \begin{pmatrix} \mathcal{L} - \boldsymbol{\Omega} \cdot \mathbf{L} & g\Psi^2(\mathbf{r}) \\ -g\Psi^{*2}(\mathbf{r}) & -[\mathcal{L} - \boldsymbol{\Omega} \cdot \mathbf{L}]^* \end{pmatrix} \quad (3.28)$$

The difference between this expression and (3.9) is the appearance of the term $-\boldsymbol{\Omega} \cdot \mathbf{L}$ in the diagonal elements. For simplicity let us consider the situation when a system is rotated about the z -axis so that the extra term is ΩL_z . Under complex conjugation this operator changes its sign making the diagonal elements different in the $\mathcal{H}_B(\text{rot})$ whereas they are identical in \mathcal{H}_B apart from an overall $-$ sign.

F. Characteristic frequency of vortex nucleation

The solution of the GP equation in the rotating frame is used to determine the characteristic frequency of vortex nucleation. The principle is the following. Let us again consider the case of a cylindrical symmetry (§III C). One determines the energies (3.12) of a condensate with and without a vortex by respectively setting κ equal to some non-zero integer and $\kappa = 0$ in the expression for Ψ . These energies are respectively denoted as $E_v(\kappa)$ and E_0 . For a static trap $E_v(\kappa)$ is always greater than E_0 . In a rotating trap at a given value of $\Omega = \Omega_{c\kappa}$, $E_v(\kappa)$ becomes the ground state energy of the hamiltonian in (3.27). The corresponding angular momentum is $\kappa\hbar N_0$ where N_0 is the number of atoms in the condensate. Therefore the characteristic rotational frequency for the nucleation of a vortex of winding number κ is given by [41]

$$\Omega_{c\kappa} = \frac{E_v(\kappa) - E_0}{N_0\kappa\hbar} \quad (3.29)$$

The ground state energy of the hamiltonian is also the minima of the thermodynamic free energy. Thus this frequency is also called the thermodynamic frequency of vortex nucleation since it is determined by minimizing the thermodynamic free energy. Using this formula Dalfovo *et. al.* [41, 42] evaluated numerically the critical frequency of vortex nucleation. Their treatment of the full GP equation (3.10) includes the effect of the confinement as well

as that of the interaction. To understand the effect of each of these terms we start with the case where both the interaction and the confinement are neglected and then subsequently include their effect in steps.

- **Non-interacting case**

To describe the non-interacting case [37] we choose again the geometry of an infinitely long cylinder. There the superfluid flow is irrotational (3.18), if the magnitude of velocity varies as

$$\mathbf{v}_s = \frac{c}{r} \hat{\theta} \quad (3.30)$$

where c is a constant. The above equation is valid for large distances. For small distances *i. e.* when r becomes comparable to the healing length ξ (3.16), v_s varies rapidly and this definition is no longer valid. The quantization of circulation (§III C) determines the constant c to be

$$v_s = \frac{\kappa \hbar}{mr} \quad (3.31)$$

If the radius of the cylinder is b , the kinetic energy per unit length along the cylinder axis is given by

$$E_v(\kappa) = \int_0^b 2\pi r dr \frac{\rho m}{2} v_s^2 = \frac{\pi \rho}{m} \kappa^2 \hbar^2 \int_0^b \frac{dr}{r} = \frac{\pi \rho}{m} \kappa^2 \hbar^2 \log \frac{b}{\xi} \quad (3.32)$$

The integral is divergent. It is regulated by using a finite cut-off ξ at the lower limit of r . This is because in presence of vortex the density ρ vanishes at the origin at a rate faster than r . The total angular momentum density per unit length of the cylinder is $\rho \pi b^2 \kappa \hbar$. Setting $\kappa = 1$ and using (3.29) one gets the thermodynamic frequency for the nucleation of the first vortex [40]

$$\Omega_{c1} = \frac{\hbar}{mb^2} \log \frac{b}{\xi} \quad (3.33)$$

- **Uniform condensate (unconfined) with interaction**

Now let us consider an uniform gas of interacting bosons without confining potential V_{tr} . The geometry is again a cylinder with radius b . We evaluate the energy of the condensate in the presence of a vortex relative to the vortex free condensate with the same number of particles. The condensate wavefunction is given in (4.15) and because of the symmetry along z -axis and very low temperature it is justified to consider both the condensate and

the vortex state correspond to $k_z = 0$. The extra energy per unit length of the vortex with $\kappa = 1$ (3.12) (chapter 9 of [4]).

$$\begin{aligned} E_v &= \int_0^b 2\pi r dr \left[\frac{\hbar^2}{2m} |\nabla \Psi(\mathbf{r})|^2 + g |\Psi(\mathbf{r})|^4 \right] - E_0 \\ &= \int_0^b 2\pi r dr \left[\frac{\hbar^2}{2m} \left(\left[\frac{d\Psi(r)}{dr} \right]^2 + \frac{\Psi(r)^2}{r^2} \right) + g |\Psi(\mathbf{r})|^4 \right] - E_0 \end{aligned} \quad (3.34)$$

Here E_0 is the energy of the bare condensate. This was evaluated first by Ginzburg and Pitaevskii [39] by using the solution of the GP equation (3.10) and the result is (for $\kappa = 1$)

$$E_v = \pi \rho \frac{\hbar^2}{m} \log \left(1.464 \frac{b}{\xi} \right) \quad (3.35)$$

where ρ corresponds to the vortex free uniform density of the condensate. In comparison to the expression (3.32) here we can see an extra factor 1.464 which accounts for the interaction among bosons. The corresponding characteristic frequency of the first vortex nucleation is

$$\Omega_{c1} = \frac{\hbar}{mb^2} \log \frac{1.464b}{\xi} \quad (3.36)$$

The calculation is detailed in the chapter 9 of [4] and the chapter 5 of [5].

• Ω_{c1} from the GP equation

The method adopted in [41, 42] by Dalfonso *et. al.* to evaluate the characteristic frequency for the vortex nucleation for a trapped non-uniform condensate from the GP equation is very similar to the one described for the uniform interacting condensate. They use a geometry with an axial symmetry (§II C). For a given number of particles in the condensate (N_0) they solve numerically the GP equation to obtain the condensate wavefunction $\Psi(\mathbf{r})$ in the presence of a vortex with winding number κ and then use the solution to evaluate the energy functional (3.12). The characteristic frequency is obtained from the relation (3.29). In their work [41] $\frac{\Omega_{c1}}{\omega_{\perp}}$ is plotted as a function of N_0 . For $N_0 = 1$ the result gives back $\Omega_{c1} = \omega_{\perp}$, which is the result for a set of non-interacting bosons and can be obtained from the solutions of the linear (single boson) Schrödinger equation (2.21). For $N_0 > 1$, because of the finite interaction present among bosons, the ratio $\frac{\Omega_{c1}}{\omega_{\perp}}$ is smaller than 1 making it possible for trapped condensate to have a vortex. A numerical investigation of the characteristic nucleation frequency and angular momentum for a multiple vortex configuration was subsequently done by Butts and Rokshar [43].

The reason for the reduction of Ω_{c1} in the presence of interactions can be understood as follows [43]. In an axially symmetric geometry and using the basis of the single particle states having definite angular momentum (2.15) (for simplicity we keep the quantum numbers n and n_z fixed) the condensate wavefunction can be expanded as

$$\Psi(\mathbf{r}) = \sum_{l_z=0}^{\infty} C_{l_z} \phi_{l_z} \quad (3.37)$$

The coefficient C_{l_z} has to be fixed variationally by extremizing the following GP energy functional (3.12) in the rotating frame

$$E_{GP}(\Omega) = \int d\mathbf{r} \left[\frac{\hbar^2}{2m} |\nabla \Psi(\mathbf{r})|^2 + V_{tr}(\mathbf{r}) |\Psi(\mathbf{r})|^2 + \frac{g}{2} |\Psi(\mathbf{r})|^4 - \Psi(\mathbf{r})^* \Omega L_z \Psi(\mathbf{r}) \right] \quad (3.38)$$

To obtain the energy of a vortex state with winding number κ this extremization has to be done with the constraint for the vorticity of the condensate wavefunction, namely

$$\sum_{l_z} |C_{l_z}|^2 l_z = \kappa \quad (3.39)$$

For a state with no vortex the only way to satisfy this constraint is to make $C_{l_z} = 0$ for $l_z \neq 0$ in (3.37). For $\kappa \neq 0$, however it is possible to make $C_{l_z} \neq 0$ for more than one value of l_z provided it is energetically favored. For non-interacting bosons (2.16), such an option is energetically ruled out upto $\Omega = \omega_{\perp}$. But for a set of bosons interacting via the contact interaction (3.1) occupying more than one angular momentum orbits reduces the interaction energy greatly. Therefore a vortex state becomes preferable as soon as the reduction in the interaction energy due to such distribution offsets the gain in the single particle energy (2.16) due to the occupation of the higher l_z states. As a result a vortex can be nucleated for $\Omega < \omega_{\perp}$. Later we shall show how an analytical expression for Ω_{c1} is obtained in the strongly interacting limit that agrees very well with the result of [41, 42] for large N_0 .

IV. GROSS-PITAEVSKII EQUATION AND ITS LINEAR STABILITY ANALYSIS

In the section §III D we have discussed the thermodynamic stability of the condensate wavefunction Ψ and mentioned that it is related to a dynamic stability. To check the dynamic stability of a solution a linear stability analysis of a steady state solution of the time-dependent GP equation (3.11) has to be performed. [7, 22, 24, 26, 27, 47]. Such an analysis

also gives the linear response of the condensate to an external perturbation. Particularly the dynamical instability associated with a particular type of steady state solution leads to the vortex nucleation as we shall see. In the following section we describe the linear stability analysis.

A. Linear response analysis of the Gross-Pitaevskii equation

Let us consider the effect of adding a weak, sinusoidal perturbation to the trap potential. Following Edwards *et.al.* [22] one can write the time-dependent GP equation (3.11) under such weak perturbation

$$i\hbar \frac{\partial \Psi(\mathbf{r}, t)}{\partial t} = \left[\left(-\frac{\hbar^2}{2m} \nabla^2 + V_{tr}(\mathbf{r}) + f_+(\mathbf{r}) \exp(-i\omega_p t) + f_-(\mathbf{r}) \exp(+i\omega_p t) \right) \right] \Psi(\mathbf{r}, t) \quad (4.1)$$

where f_{\pm} and ω_p are respectively the amplitudes and the frequency of the sinusoidal perturbation. Since it is weak one assumes that the deviation from the solution of the unperturbed GP equation is also going to be small and can be written under the form

$$\Psi(\mathbf{r}, t) = \exp(-i\mu t) [\Psi(\mathbf{r}) + \delta\Psi(\mathbf{r}, t)] \quad (4.2)$$

with $\delta\Psi = u(\mathbf{r}) \exp(-i\omega_p t) + v(\mathbf{r})^* \exp(i\omega_p t)$.

After inserting Eq. (4.2) into Eq. (4.1) and keeping terms which are linear in $u(\mathbf{r}), v(\mathbf{r}), f_{\pm}(\mathbf{r})$ one gets

$$\mathcal{H}_B \begin{pmatrix} u(\mathbf{r}) \\ v(\mathbf{r}) \end{pmatrix} = \begin{pmatrix} \Psi(\mathbf{r}) f_+(\mathbf{r}) \\ \Psi^*(\mathbf{r}) f_-^*(\mathbf{r}) \end{pmatrix} \quad (4.3)$$

The Bogoliubov hamiltonian \mathcal{H}_B therefore appears in the linear stability analysis. The equations which determine the time evolution of the small fluctuations u and v are identical to the equations (3.23) (after $f_{\pm}(\mathbf{r})$ is set to zero and after changing p into λ). The linearized evolution of the non-condensed part of the Bose-field operator $\delta\hat{\psi}(\mathbf{r})$ which has been discussed earlier (section §III D) is therefore formally equivalent to the linearized response of the condensate to a classical perturbation. Using Eq. (3.11).

$$i\hbar \frac{\partial}{\partial t} \begin{pmatrix} u_{\lambda}(\mathbf{r}) \\ v_{\lambda}(\mathbf{r}) \end{pmatrix} = \mathcal{H}_B \begin{pmatrix} u_{\lambda}(\mathbf{r}) \\ v_{\lambda}(\mathbf{r}) \end{pmatrix} = \hbar\omega_{\lambda} \begin{pmatrix} u_{\lambda}(\mathbf{r}) \\ v_{\lambda}(\mathbf{r}) \end{pmatrix} \quad (4.4)$$

The time evolution of these modes is given by $e^{-i\omega_\lambda t}$. This factor remains bounded in time provided that the imaginary part of ω_λ is negative. This leads to the dynamic stability condition that for all ω_λ $Im(\omega_\lambda) \leq 0$. Since the condensate wavefunction in a steady state is obtained by finding the local minima of the GP energy functional it can be shown that the dynamic stability criterion is more stringent and requires [63] $Im(\omega_\lambda) = 0$. Using the normalization condition for Bogoliubov wavevectors u_λ and v_λ one can write the condensate response to an arbitrary small perturbation $f(\mathbf{r})$ of frequency ω_p as [22]

$$\begin{pmatrix} u(\mathbf{r}) \\ v(\mathbf{r}) \end{pmatrix} = \sum_\lambda \frac{g_\lambda}{\hbar(\omega_\lambda - \omega_p)} \begin{pmatrix} u_\lambda(\mathbf{r}) \\ v_\lambda(\mathbf{r}) \end{pmatrix} \quad (4.5)$$

where

$$g_\lambda = \int d\mathbf{r} f(\mathbf{r}) [\Psi(\mathbf{r}) u_\lambda^*(\mathbf{r}) + \Psi^*(\mathbf{r}) v_\lambda^*(\mathbf{r})] \quad (4.6)$$

In the next section we shall describe how these normal modes of the Bogoliubov hamiltonian are calculated for a set of interacting bosons without any confinement which gives the usual Bogoliubov dispersion law. This is a standard text-book material and is given in many references. For example see [4, 5, 7].

B. Condensate in a box

The atoms are trapped in a cubic box of size L , and we assume periodic boundary conditions. Solutions of the stationary Gross-Pitaevskii equation (3.10) can be written as plane waves with vanishing momentum,

$$\Phi_0(\mathbf{r}) = \frac{1}{L^{3/2}} \exp(i\mathbf{k} \cdot \mathbf{r})|_{\mathbf{k}=0} \quad (4.7)$$

with the chemical potential $\mu = gN_0|\phi_0|^2 = \rho_0 g$ and the density of the condensate atoms $\rho_0 = N_0/L^3$. In the absence of any confinement the Bogoliubov hamiltonian \mathcal{H}_B is translational invariant. Therefore one seeks its eigenvectors in the form of plane waves.

$$\begin{pmatrix} u_\mathbf{k}(\mathbf{r}) \\ v_\mathbf{k}(\mathbf{r}) \end{pmatrix} = \frac{e^{i\mathbf{k} \cdot \mathbf{r}}}{L^{3/2}} \begin{pmatrix} U_\mathbf{k} \\ V_\mathbf{k} \end{pmatrix}. \quad (4.8)$$

\mathcal{H}_B can be written in a block-diagonal form with each block (2×2 matrix) corresponding to a given wave vector \mathbf{k} .

$$\mathcal{H}_B[\mathbf{k}] = \begin{pmatrix} \left[\frac{\hbar^2 k^2}{2m} + \rho_0 g \right] & \rho_0 g \\ -\rho_0 g & -\left[\frac{\hbar^2 k^2}{2m} + \rho_0 g \right] \end{pmatrix}. \quad (4.9)$$

This matrix can be diagonalized, giving one eigenvector with the positive eigenvalue $\epsilon_{\mathbf{k}}$ and one eigenvector with negative eigenvalue $-\epsilon_{\mathbf{k}}$ where

$$\epsilon_{\mathbf{k}} = \left[\frac{\hbar^2 k^2}{2m} \left(\frac{\hbar^2 k^2}{2m} + 2\rho_0 g \right) \right]^{1/2} \quad (4.10)$$

The spectrum (4.10) was first derived by Bogoliubov. Here only the case for the repulsive bosons ($g > 0$) is considered. For attractive bosons ($g < 0$) the spectrum exhibits a different behaviour. The Bogoliubov spectrum of repulsively interacting Bose gas strongly differs from those of a free Bose gas particularly for small k . Here the spectrum is linear and neglecting the quadratic term in (4.10) one gets

$$\epsilon_{\mathbf{k}} \simeq \hbar k \sqrt{\frac{\rho_0 g}{m}}. \quad (4.11)$$

This corresponds to a spectrum of sound-waves propagating with a sound velocity c_s given by

$$c_s = \frac{d\omega_{\vec{k}}}{dk} = \frac{1}{\hbar} \frac{d\epsilon_{\vec{k}}}{dk} = \sqrt{\frac{\rho_0 g}{m}} \quad (4.12)$$

It is this linear part of the spectrum which differentiates the behaviour of an interacting Bose gas from that of a free Bose gas. For large k the spectrum is quadratic like that of a free Bose gas.

C. Thermodynamic instability of a vortex solution

Dodd *et. al.* [24] carried out the linear stability analysis of the condensate with a vortex (with $\kappa = 1$) and find out that the corresponding Bogoliubov spectrum differs significantly in terms of the excitation frequency from Bogoliubov spectrum for the condensate without a vortex. Apart from providing the clue for the spectroscopic signature of the presence of a vortex their calculation also revealed the presence of a mode with negative energy and positive normalization in the spectrum which suggests that the vortex solution is dynamically

unstable. Rokshar [25] (see also [31]) explained this instability by pointing out that a Bogoliubov quasiparticle feels an effective potential which is approximately of the form (see the diagonal term of \mathcal{H}_B)

$$V_{eff} = V_{tr} + 2g|\Psi(\mathbf{r})|^2 - \mu \quad (4.13)$$

where $\Psi(\mathbf{r})$ is the condensate wavefunction with a vortex. Since the condensate density vanishes at the core of a vortex and the confinement potential also reaches its minimum there, V_{eff} can be negative in the core (relative to the chemical potential) forming a bound core state. The quasiparticles are also bosons. So the occupation of this bound state can be macroscopic and all the particles which form a vortex can be transferred to this core state. As a result the vortex collapses. For non-interacting bosons this can be easily verified since the core state is nothing but the ground state which has always a lower energy than the vortex state for a confined system (see the discussion in sec. §IID). This has been verified by Dodd *et. al.* [24] by showing that in the limit of zero interaction, the energy corresponding to this mode approaches the value $-\hbar\omega_{\perp}$. The minus sign occurs since the energy is measured with respect to the vortex energy. Therefore in a static trap a vortex state is always thermodynamically as well as dynamically unstable.

Before pointing out how this instability can be removed we briefly describe how Bogoliubov modes are calculated for a trapped condensate with or without a vortex. This has been done by several groups [22, 24, 27, 28, 32, 47] using various schemes to study the stability properties of the condensate and its vortices.

Let us assume that the atomic cloud is trapped in a cylindrical trap. This happens when the aspect ratio (2.13) $\lambda_R \ll 1$ such that the confinement potential is given by

$$V_{tr}(\mathbf{r}) = \frac{1}{2}m\omega_{\perp}^2(r^2 + \lambda_R^2 z^2) \approx \frac{1}{2}m\omega_{\perp}^2 r^2 \quad (4.14)$$

and periodic boundary conditions are imposed along the z direction. The condensate wave function is written in the form:

$$\Psi(\mathbf{r}) = \Psi(r, \theta, z) = \Psi(r)e^{i\kappa\theta}e^{ik_z z} \quad (4.15)$$

The winding number κ (§III C) is finite when a vortex is present and vanishes in the absence of a vortex. Since the trap is axisymmetric

$$u_{\lambda}(\mathbf{r}) = u_{\lambda}(r)e^{ik_z z}e^{i(l_z + \kappa)\theta} \quad (4.16)$$

$$v_{\lambda}(\mathbf{r}) = v_{\lambda}(r)e^{ik_z z}e^{i(l_z - \kappa)\theta}. \quad (4.17)$$

The quantum numbers $\mathbf{n} = (n, l_z, k_z)$ may take the following values: $n \in \mathbf{N}$; $l_z \in \mathbf{Z}$; and $k_z = q \frac{2\pi}{L}$, $q \in \mathbf{Z}$, where L is the length of the cylinder.

First we solve the GP equation with the ansatz (4.15) and then we diagonalize the Bogoliubov matrix \mathcal{H}_B with that solution after expanding $u_\lambda(r)$ and $v_\lambda(r)$ in a suitable basis. This has been detailed in a number of references (for example see [22, 28]). Since the normal modes are eigenfunctions of the angular momentum operator L_z , according to (4.17) if $u_\lambda(\mathbf{r})$ is an eigenfunction of L_z with a particular eigenvalue l_z^u (in the unit of \hbar), then $v_\lambda(\mathbf{r})$ will be also an eigenfunction of L_z with eigenvalue $l_z^u - 2\kappa$.

We shall now describe how we can stabilize a vortex solution. Following Fetter and Svidzinsky [18] we denote the anomalous mode frequency as ω_a . One way of stabilizing this mode is to rotate the condensate [18, 30]. Let us consider an axisymmetric condensate in rotational equilibrium at an angular velocity Ω around the z -axis. Since in the rotating frame, the hamiltonian is $H - \Omega L_z$, and the Bogoliubov amplitudes have frequencies $\omega_\lambda(\Omega) = \omega_\lambda - l_z \Omega$, where ω_λ is the frequency in the non-rotating frame and l_z is the angular momentum quantum number. It has been found in [24] that for the anomalous mode $l_z = -1$. The resulting frequency in the rotating frame is

$$\omega_a(\Omega) = \omega_a + \Omega, \quad (4.18)$$

Since ω_a is negative, the anomalous frequency in a rotating frame increases linearly towards zero with increasing Ω and particularly $\omega_a(\Omega)$ vanishes at a characteristic rotation frequency

$$\Omega_{c1} = -\omega_a = |\omega_a| \quad (4.19)$$

which implies that for $\Omega \geq \Omega_{c1}$ the singly quantized vortex becomes locally stable. Linn and Fetter [45] carried out an explicit perturbative analysis to confirm this directly from the GP equation. One can also stabilize the vortex solution by increasing temperature and also by putting disorder which will pin the vortices[30]. The dependence of the vortex stability on rotation and temperature are combined to give a phase diagram for the vortices [30, 64].

V. APPROXIMATION SCHEMES TO STUDY THE BEHAVIOUR OF THE CONDENSATE

The Bogoliubov theory gives a very accurate description of the trapped BEC near the zero temperature, in terms of the condensate wavefunction $\Psi(\mathbf{r})$ and a set of collective excitations. It also tells whether a state represented by the condensate wavefunction is stable or not. Present experiments are done under conditions where further simplifications of this theory is possible. This enables us to interpret different experimentally measurable properties in terms of the known system parameters, like the number of atoms in the condensate N_0 , the interaction strength (a) etc. We shall now discuss these approximation schemes in some detail.

For further approximation one notes that depending on the parameters such as the number of atoms (N_0) present, the trap frequency etc. the role of interaction in determining the properties of an atomic condensate can be different [40, 41]. For the trapped condensate this was first pointed out by Baym and Pethick [40] and subsequently verified numerically by Dalfonso and Stringari [41]. We start with the following Gaussian variational ansatz for an isotropic confinement (the present derivation follows a review by Castin [7])

$$\Psi(\mathbf{r}) = \frac{1}{\pi^{3/4} R^{3/2}} e^{-r^2/2R^2} \quad (5.1)$$

where the spatial width R is the only variational parameter. After substitution in (3.12) this gives the following mean energy per particle

$$\bar{e} \equiv \frac{H[\Psi, \Psi^*]}{N_0} = \frac{3\hbar^2}{4mR^2} + \frac{3}{4}m\omega^2R^2 + \frac{\hbar^2 N_0 a}{m R^3} \frac{1}{\sqrt{2\pi}} \quad (5.2)$$

Setting the unit of length to $\frac{1}{\sqrt{b_\omega}} = (\hbar/m\omega)^{1/2}$ and that of energy to $\hbar\omega$ one obtains:

$$\bar{e} = \frac{3}{4} \left[\frac{1}{R^2} + R^2 \right] + \frac{\chi}{2R^3} \quad (5.3)$$

with

$$\chi = \sqrt{\frac{2}{\pi}} \frac{N_0 a}{\sqrt{\hbar/m\omega}}. \quad (5.4)$$

The kinetic energy term scales like $1/R^2$, whereas the energy due to the confinement potential scales as R^2 . Since N_0/R^3 is the density of atoms in the condensate, parameter χ ($\propto N_0 a$) measures the effect of the interactions on the condensate density. The case $\chi \ll 1$ corresponds to the weakly interacting regime, close to the ideal Bose gas limit $\chi = 0$; the case $\chi \gg 1$ corresponds to the strongly interacting regime.

A. The Thomas-Fermi approximation for an isotropic confinement

When $\chi \gg 1$ the condensate can be well described by the Thomas-Fermi (TF) approximation. Since $b_\omega = 1$, $\chi \gg 1 \equiv N_0 a \gg 1$. If N_0 is now increased, to minimize the energy (5.3) R will take a larger value. The size of the condensate R becomes larger and the kinetic energy term becomes less important compared to other terms since

$$\begin{aligned} R &\gg 1/\sqrt{b_\omega} \\ \Rightarrow \frac{E_{\text{kin}}}{E_{\text{harm}}} &\simeq \frac{\frac{\hbar^2}{mR^2}}{m\omega^2 R^2} \simeq \left(\frac{\hbar}{m\omega R^2}\right)^2 \ll 1 \end{aligned} \quad (5.5)$$

This result should be contrasted against that of the noninteracting case for which the ratio is 1. Therefore the kinetic energy term in the GP equation (3.10) can be neglected in this limit. This is known as the Thomas-Fermi (TF) approximation. We emphasize that TF regime is called strongly interacting, not due to a larger value of the s -wave scattering length a , but for the dominant role played by the interaction energy in comparison to the kinetic energy. The Thomas-Fermi radius R which gives the size of the system in this limit, can then be obtained by equating the energy due to the confinement potential and the repulsive interaction energy. The TF approximation leads to

$$\mu_{TF}\Psi(\mathbf{r}) \simeq V_{tr}(\mathbf{r})\Psi(\mathbf{r}) + g|\Psi(\mathbf{r})|^2\Psi(\mathbf{r}). \quad (5.6)$$

$$\Rightarrow \Psi(\mathbf{r}) = \left(\frac{\mu_{TF} - V_{tr}(\mathbf{r})}{g}\right)^{1/2} \quad (5.7)$$

The chemical potential can now be expressed in terms of the other system parameters from the normalization condition $\int d\mathbf{r}|\Psi(\mathbf{r})|^2 = N_0$ where the domain of integration is limited by the Thomas-Fermi radius R which is then determined from the boundary condition $\Psi(\mathbf{r}) = 0$ for $r \geq R$ which yields

$$\mu_{TF} = \frac{1}{2}m\omega^2 R^2 \quad (5.8)$$

Therefore the TF approximation determines the chemical potential μ_{TF} and the size of the cloud R in terms of m , ω , g , N_0 which are all known parameters. The ground state condensate wavefunction $\Psi(\mathbf{r})$ is consequently determined as a real valued quantity which vanishes sharply at the boundary $r = R$. However (see §III C) $\Psi(\mathbf{r})$ is generally a complex valued function which can be written as $\Psi(\mathbf{r}) = \sqrt{\rho(\mathbf{r})}e^{iS(\mathbf{r})}$.

B. Non-isotropic traps

For a non-isotropic harmonic confining potential (§II A) the boundary condition (5.8) yields the shape of the condensate as being that of an ellipsoid of radius R_α along the axis α

$$R_\alpha^2 = \frac{2\mu_{TF}}{m\omega_\alpha} \quad (5.9)$$

where $\alpha = x, y, z$. Using the same method as in the case of an isotropic confinement the condensate density and the chemical potential can be determined in terms of the system parameters such as N_0 , a and ω_α , giving respectively

$$\rho(r) = |\Psi_{TF}(\mathbf{r})|^2 = \frac{1}{g} [\mu_{TF} - V_{tr}(\mathbf{r})] \Theta [\mu_{TF} - V_{tr}(\mathbf{r})] = \rho(0) \left(1 - \sum_\alpha \frac{r_\alpha^2}{R_\alpha^2}\right) \Theta \left(1 - \sum_\alpha \frac{r_\alpha^2}{R_\alpha^2}\right), \quad (5.10)$$

$$\mu_{TF} = \frac{1}{2} \hbar \bar{\omega} \left[15 \frac{N_0 a}{(\hbar/m\bar{\omega})^{1/2}} \right]^{2/5} = \frac{1}{2} \hbar \bar{\omega} \frac{R_{TF}^2}{\bar{a}^2} \quad (5.11)$$

where $\bar{\omega} = (\omega_x \omega_y \omega_z)^{1/3}$, $\bar{a} = \frac{1}{\sqrt{b\bar{\omega}}} = \sqrt{\frac{\hbar}{m\bar{\omega}}}$, and the mean TF radius $R_{TF} = \prod_\alpha (R_\alpha)^{1/3}$. In the TF regime, since $\chi \gg 1$, the chemical potential μ_{TF} satisfies

$$\mu_{TF} \gg \hbar \bar{\omega}, \quad (5.12)$$

At the center of the TF ellipsoid ($x, y, z = 0$) the density (5.10) is maximum and it is given as

$$\rho(0) = \frac{\mu_{TF}}{g} \quad (5.13)$$

Unlike for an unbounded and uniform condensate, in a trapped non-uniform condensate the healing length (3.16) can only be defined in terms of a density at a reference point. Conventionally it is chosen as $\rho(0)$, the TF density at the center of the condensate. Therefore we set $\xi = \xi_0 = [8\pi\rho(0) a]^{-1/2}$. This leads to the following relation between the TF chemical potential (5.13) and the healing length

$$\frac{\hbar^2}{2m\xi_0^2} = g\rho(0) = \mu_{TF} \quad (5.14)$$

Once the healing length is defined, the relation among different length scales in the TF regime can be determined from the relation

$$\xi R_{TF} = \bar{a}^2 \quad (5.15)$$

Since in the TF regime $\frac{R_{TF}}{\bar{a}} \gg 1$, one has

$$\frac{\xi}{\bar{a}} = \frac{\bar{a}}{R_{TF}} \ll 1. \quad (5.16)$$

ξ_0 (3.16) gives the size of a vortex core. This can be checked from the GP equation. A small healing length ξ_0 characterizes a small vortex core. In contrast, the healing length (and the vortex-core radius) in the ideal Bose gas limit are comparable with \bar{a} and hence with the size of the condensate.

The TF approximation (5.5) breaks down at the boundary of the TF region where the density $|\Psi(\mathbf{r})|^2$ drops to zero (5.7-5.8). The realistic wavefunction which can be obtained from the solution of full Gross-Pitaevskii equation [41] has a rounded-off tail which vanishes exponentially. In the large r region (near boundary) the density is very low and therefore the kinetic energy cannot be any longer neglected compared to the interaction energy term ($\equiv \rho(\mathbf{r})^2$) in the expression (3.12). The modification due to this non-negligible kinetic energy will be discussed briefly in a later section (see §IX B).

VI. VORTEX SOLUTION IN THE THOMAS-FERMI REGIME

We shall now study the vortex solution under the TF expression. We consider the case where the trap has an axis of symmetry, namely $\omega_x = \omega_y = \omega_\perp$ (§II C). In such a geometry the TF radius in the $x - y$ plane is given by $R_x = R_y = R_\perp$. The condensate wavefunction in this case is of the form (see section §III C)

$$\Psi = |\Psi(\mathbf{r})| e^{iS(\mathbf{r})} \quad (6.1)$$

In the cylindrical polar co-ordinate (r, θ, z) one again sets $S = \kappa\theta$, so that

$$\mathbf{v}_s = \frac{\hbar}{mr} \kappa \hat{\theta}, \quad (6.2)$$

Using the harmonic oscillator length scales $a_\perp = 1/\sqrt{b_{\omega_\perp}}$ and $a_z = 1/\sqrt{b_z}$ and the harmonic oscillator energy scale $\hbar\omega_\perp$ first we write the GP equation (3.10) in a dimensionless form

$$\left[-\frac{\hbar^2}{2m} \left[\frac{\partial}{\partial r} \left(r \frac{\partial}{\partial r} \right) + \frac{\kappa^2}{r^2} \right] + \frac{1}{2} m \omega_\perp^2 (r^2 + \lambda_R^2 z^2) + g |\Psi(\mathbf{r})|^2 \right] \Psi(\mathbf{r}) = \mu \Psi(\mathbf{r}) \quad (6.3)$$

Due to the presence of the centrifugal term, the solution of this equation for $\kappa \neq 0$ has to vanish on the z -axis. From the asymptotic behaviour of the Eq. (6.3) near the origin

it can be verified that the region over which the density changes very fast to zero is given by the healing length ξ_0 . Therefore in this region the kinetic energy cannot be neglected. Away from the origin the density profile is going to be same as the TF density without a vortex. The TF approximation can now be applied by neglecting the radial part of the kinetic energy (since it is sub-dominant relative to the centrifugal term for small r) which gives the following TF density profile [27]

$$\rho_\kappa \approx \rho(0) \left(1 - \frac{\kappa^2 \xi_0^2}{r^2} - \frac{r^2}{R_\perp^2} - \frac{z^2}{R_z^2} \right) \Theta \left(1 - \frac{\kappa^2 \xi_0^2}{r^2} - \frac{r^2}{R_\perp^2} - \frac{z^2}{R_z^2} \right) \quad (6.4)$$

where we have used the relation (5.14) assuming that the correction to the μ_{TF} due to the presence of a vortex can be neglected [47]. Thus the density profile of a vortex in TF approximation significantly differs from the ground state density profile only over a length scale ξ_0 .

A. Critical frequency of vortex nucleation in the TF approximation

The calculation for the critical frequency under TF approximation was carried on by Lundh *et. al.* [46], Sinha [47] and Feder [48]. The following discussion closely follows [46]. The method consists in evaluating the extra energy associated with the presence of a vortex and then divide it by the total angular momentum, both determined within the TF approximation. The ratio then gives the critical frequency. Once there is a finite confinement along the z direction the system is not exactly like a infinite cylinder. But if the aspect ratio (2.13) $\lambda_R \ll 1$, a cylindrical profile of the trap is still a good approximation.

First one assumes that the TF radius satisfies the condition $R_\perp \ll R_z$. To obtain the energy of a vortex, Lundh *et. al.* [46] proposes that for such a large condensate the domain of integration in the transverse plane can be divided into two parts. In the region having a radius r_i such that $\xi \ll r_i \ll R_\perp$ one can use the expression (3.35) after replacing b for r_i and for the region $r_i < r < R_\perp$ one obtains the energy by integrating the kinetic energy term (interaction is neglected since the density is low in this region). This gives the energy of a vortex ($\kappa = 1$) per unit length as

$$\begin{aligned} E_v &= \pi \rho(0) \frac{\hbar^2}{m} \log \left(1.464 \frac{r_i}{\xi_0} \right) + \frac{1}{2} \int_{r_i}^{R_\perp} 2\pi r dr m \rho(r) v_s^2(r) \\ &\approx \pi \rho(0) \frac{\hbar^2}{m} \log \left(\frac{0.888 R_\perp}{\xi_0} \right) \end{aligned} \quad (6.5)$$

In the second integral we use the ground state TF density (5.10) since in this domain it is $\approx \rho_1$ (6.4).

The total angular momentum for a vortex state with $\kappa = 1$ in the TF approximation is given by

$$L_z = \hbar \left[\rho(0) \int_0^{R_\perp} \left(1 - \frac{r^2}{R_\perp^2}\right) 2\pi r dr \right] = \frac{1}{2} \hbar \rho(0) \pi R_\perp^2 \quad (6.6)$$

The critical frequency is therefore

$$\Omega_{c1} = 2 \frac{\hbar}{m R_\perp^2} \log \left(\frac{0.888 R_\perp}{\xi_0} \right) \quad (6.7)$$

Energy of the condensate with a vortex is always measured relatively to the energy of the bare condensate. The energies due to the harmonic confinement ($\frac{1}{2} m \omega_\perp^2 r^2 \rho$) for these two cases differ appreciably from each other for $r < \xi_0$. Hence its contribution is neglected in the above derivation.

The next correction to the formula of the characteristic nucleation frequency comes by assuming the TF radius along the z direction is finite. As mentioned earlier the shape of the cloud in this case is that of an ellipsoid and as a result its TF radius in the $x - y$ plane is z dependent. The energy for a vortex in this case can be obtained by integrating the energy of a vortex state per unit length in two-dimension (6.5) along the z -axis from $-R_z$ to R_z after replacing R_\perp by $R_\perp(z) = R_\perp(1 - \frac{z^2}{R_z^2})$. Such a calculation yields the following expressions:

$$E_v = \rho(0) \frac{\pi \hbar^2}{m} \int_{-R_z}^{R_z} dz \left(1 - \frac{z^2}{R_z^2}\right) \log \left(\frac{0.888 R_\perp}{\xi_0} \left(1 - \frac{z^2}{R_z^2}\right) \right) = \frac{4\pi \rho(0) \hbar^2}{3} \frac{R_z}{m} \log \left(\frac{0.671 R_\perp}{\xi_0} \right) \quad (6.8)$$

$$L_z = \hbar \left[\rho(0) \int_{-R_z}^{R_z} \left(1 - \frac{r^2}{R_\perp^2} - \frac{z^2}{R_z^2}\right) dz 2\pi r dr \right] = \frac{8\pi}{15} \hbar \rho(0) \pi R_\perp^2 R_z \quad (6.9)$$

$$\Omega_{c1} = \frac{E_v}{L_z} = \frac{5}{2} \frac{\hbar}{m R_\perp^2} \log \left(\frac{0.671 R_\perp}{\xi_0} \right) \quad (6.10)$$

Within this approximation it is important to note that for such an axisymmetric vortex the critical frequency does not depend on the TF radius along the axis of symmetry, though however the change in the shape of the cloud influences the absolute value of the critical frequency. This ends our discussion about the static properties of a TF (large) condensate. We shall now switch over to the description of the dynamic extension of this approximation.

VII. HYDRODYNAMIC THEORY OF THE CONDENSATE

The study of a large (or equivalently strongly interacting) condensate can be extended to the time-dependent situations by formulating a hydrodynamic theory of the condensate. The hydrodynamic equations [49] describes the time evolution of the density and the velocity field of the condensate. Vortex nucleation in a rotating trapped condensate is a dynamic process. Therefore the time-evolution of the density and the associated velocity field plays a pivotal role in the nucleation mechanism. For a large and strongly interacting condensate (TF limit) these hydrodynamic equations are identical to the Euler equations of the classical hydrodynamics. A linear stability analysis of the hydrodynamic equations of the condensate [49] gives a description of the collective excitations in terms of the density fluctuations and the associated velocity fields.

We shall see in the following discussion that one actually gets an analytical description of this collective excitations using this classical hydrodynamic theory. Since the Bogoliubov theory also describes the collective excitations one may ask how the collective excitations of the the hydrodynamic theory are related to the Bogoliubov excitations. Applying the TF approximation directly to the Bogoliubov equations through a large N_0 expansion Sinha [47] (see also [27]) showed that the dispersion law [49] for the collective excitations obtained under classical hydrodynamic approximation can be reproduced. The hydrodynamic theory of the condensate has been discussed in a number of references and has also been reviewed in [4, 6, 7, 18]. We discuss it in the following section briefly.

A. Time evolution of the condensate density and velocity

To enable the construction of a hydrodynamic theory of the condensate the wavefunction $\Psi(\mathbf{r})$ can be split into a modulus and a phase

$$\Psi(\mathbf{r}) = \sqrt{\rho(\mathbf{r})} e^{i \frac{S(\mathbf{r})}{\hbar}} \quad (7.1)$$

and the condensate energy (3.12) rewrites as

$$E_{GP}[\rho, S] = \int d\mathbf{r} \left[\frac{\hbar^2}{2m} (\nabla \sqrt{\rho})^2 + \rho \frac{(\nabla S)^2}{2m} + V_{tr}\rho + \frac{g}{2} \rho^2 \right] \quad (7.2)$$

Note that here we have explicitly divided the condensate phase by \hbar . The corresponding Lagrangian is

$$L_{GP} = - \left[\rho \partial_t S + \frac{\hbar^2}{2m} (\nabla \sqrt{\rho})^2 + \rho \frac{(\nabla S)^2}{2m} + V_{tr} \rho + \frac{g}{2} \rho^2 \right]. \quad (7.3)$$

Treating $\rho(\mathbf{r}, t)$ and $S(\mathbf{r}, t)$ as generalized co-ordinates, one gets respectively the following Euler-Lagrange equations that define the full hydrodynamic theory of the condensate

$$\partial_t S + \frac{1}{2m} (\nabla S)^2 + V_{tr} + \rho g = \frac{\hbar^2}{2m} \frac{\nabla^2 \sqrt{\rho}}{\sqrt{\rho}}. \quad (7.4)$$

$$\partial_t \rho + \nabla \cdot [\rho \mathbf{v}_s] = 0. \quad (7.5)$$

with

$$\mathbf{v}_s = \frac{\mathbf{j}_{\text{proba}}}{\rho} = \frac{\hbar}{2im} [\Psi^* \nabla \Psi - \text{c.c.}] = \frac{\nabla S}{m} \quad (7.6)$$

is the local velocity field of the condensate. The equation (7.5) is the usual continuity equation. The time evolution of the velocity field is obtained by taking the gradient of both sides of the equation (7.4).

$$\begin{aligned} m \partial_t \mathbf{v}_s &= -\nabla \left[\frac{1}{2} m v_s^2 + V_{tr}(\mathbf{r}) + g \rho(\mathbf{r}) - \frac{\hbar^2}{2m} \frac{\nabla^2 \sqrt{\rho}}{\sqrt{\rho}} \right] \\ &= -\nabla \left(\frac{1}{2} m v_s^2 + \mu \right) \end{aligned} \quad (7.7)$$

where the chemical potential is defined as

$$\mu = V_{tr} + g \rho - \frac{\hbar^2}{2m} \frac{\nabla^2 \sqrt{\rho}}{\sqrt{\rho}} \quad (7.8)$$

Using the expression (5.6) the above equation can be rewritten as

$$\mu = \mu_{TF} - \frac{\hbar^2}{2m} \frac{\nabla^2 \sqrt{\rho}}{\sqrt{\rho}} \quad (7.9)$$

For a uniform BEC ($V_{tr} = 0$) at $T = 0$, the chemical potential $\mu = g \rho_0$ and the pressure $p = -\frac{\partial E}{\partial V}|_T = \frac{g}{2} \rho_0^2$. Using the same expression for pressure after replacing ρ_0 by ρ , (7.7) can be rewritten as

$$m \partial_t \mathbf{v}_s = -\nabla \left[\frac{1}{2} m v_s^2 + V_{tr}(\mathbf{r}) + \frac{\nabla p}{\rho} - \frac{\hbar^2}{2m} \frac{\nabla^2 \sqrt{\rho}}{\sqrt{\rho}} \right] \quad (7.10)$$

which is very similar to the Euler equation for classical hydrodynamics

$$m \partial_t \mathbf{v}_s = -\nabla \left[m(\mathbf{v}_s \cdot \nabla) \mathbf{v}_s + V_{tr}(\mathbf{r}) + \frac{\nabla p}{\rho} \right] \quad (7.11)$$

where we use $\nabla(\frac{1}{2}mv_s^2) = m(\mathbf{v}_s \cdot \nabla)\mathbf{v}_s$. The only exception is the so called quantum pressure term, given by

$$\mu - \mu_{TF} = -\frac{\hbar^2}{2m} \frac{\nabla^2 \sqrt{\rho}}{\sqrt{\rho}}, \quad (7.12)$$

the only term in the equations where \hbar appears. The source of this term is the kinetic energy of the condensate.

B. Classical hydrodynamic approximation

If the scale of variation of ρ is of the order of R , the pressure term in the equation (7.10) is of the order $\frac{g\rho}{mR}$ whereas the quantum pressure term (7.12) is of the order $\frac{\hbar^2}{m^2 R^3}$. Therefore the quantum pressure term can be neglected as long as $\frac{(\frac{\hbar^2}{m^2 R^3})}{(\frac{g\rho}{mR})} \ll 1$. This implies $R \gg \frac{\hbar}{\sqrt{mg\rho}}$ which finally gives the condition

$$R \gg \xi \quad (7.13)$$

This condition is satisfied for a large TF condensate (5.16). In this limit neglecting the quantum pressure term in (7.10) we get the classical hydrodynamic equation for the condensate

$$m(\partial_t + \vec{v} \cdot \nabla) \vec{v} = -\nabla[V_{tr} + g\rho]. \quad (7.14)$$

and the chemical potential μ becomes μ_{TF} .

Finally we write the classical hydrodynamic equations in a trap rotating with an angular velocity Ω

$$\partial_t \rho + \nabla \cdot [\rho(\mathbf{v}_s - \boldsymbol{\Omega} \times \mathbf{r})] = 0 \quad (7.15)$$

$$m\partial_t \mathbf{v}_s + \nabla \left[\frac{1}{2}mv_s^2 + V_{trap}(\mathbf{r}) + \frac{\nabla p}{\rho} - \mathbf{v}_s \cdot (\boldsymbol{\Omega} \times \mathbf{r}) \right] = 0 \quad (7.16)$$

C. Collective excitations from the classical hydrodynamic theory

Using the hydrodynamic equations (7.5) and (7.14) Stringari [49] studied the collective excitations of a trapped condensate. For a review see also [4, 5, 6, 7]. Let us denote the steady state (time-independent) density and velocity satisfying (7.5) and (7.14) by ρ_s and \mathbf{v}_s . We follow the method described in the section (§IV A) in order to linearize these equations

about the steady state solutions. This yields

$$\frac{\partial \delta \rho}{\partial t} + \nabla \cdot [\rho_s \delta \mathbf{v}_s] = 0 \quad (7.17)$$

$$m \frac{\partial \delta \mathbf{v}_s}{\partial t} + \nabla [\delta \rho g] = 0 \quad (7.18)$$

which gives

$$\partial_t^2 \delta \rho - \nabla \cdot [c_s^2(\mathbf{r}) \nabla \delta \rho] = 0 \quad (7.19)$$

while defining $mc_s^2(\vec{r}) = \rho_s(\mathbf{r})g$. Therefore in a non-uniform trapped condensate the collective excitations which take the form of density fluctuations propagates as sound waves with a position dependent sound velocity $c_s(\vec{r})$ unlike the collective excitations in a uniform condensate where such a sound velocity is constant (4.12). The collective mode frequencies can be obtained by writing

$$\delta \rho(\mathbf{r}, t) = \delta \rho(\mathbf{r}) e^{i\omega_{cl} t} \quad (7.20)$$

Since the steady state density is same as the TF density, *i.e.* $\rho_s = \frac{\mu_{TF} - V_{tr}(\mathbf{r})}{g}$, the eigenvalue equations are

$$-\omega_{cl}^2 \delta \rho = \frac{1}{m} [\nabla V_{tr}(\mathbf{r}) \cdot \nabla \delta \rho - (\mu_{TF} - V_{tr}(\mathbf{r})) \nabla^2 \delta \rho] \quad (7.21)$$

The solutions of these modes have been obtained by Stringari [49]. Here we mention some results which will be later used to explain the process of vortex nucleation in the current experiments.

D. Hydrodynamic Modes for trapped condensates

- Spherical trap

For the spherical trap described in (§II) Eq. (7.21) becomes

$$-\omega_{cl}^2 \delta \rho = \left[\omega^2 r \frac{\partial}{\partial r} \delta \rho - \frac{\omega^2}{2} (R^2 - r^2) \nabla^2 \delta \rho \right] \quad (7.22)$$

where R is the TF radius (5.8). The eigenvalues are given by [49]

$$\omega_{cl}^2 = (l + 3n_r + 2n_r l + 2n_r^2) \omega^2 \quad (7.23)$$

The normal modes of the density fluctuations are given in terms of the hypergeometric functions and the spherical harmonics, namely

$$\delta \rho(\mathbf{r}, t) = C r^l F(-n_r, l + n_r + \frac{3}{2}, l + \frac{3}{2}; \frac{r^2}{R^2}) Y_{l, l_z}(\theta, \phi) e^{-i\omega_{cl} t} \quad (7.24)$$

Details of this calculation is also available in chapter 7 of ref. [4]. Here n_r gives the number of radial nodes and l gives the polarity of the density oscillation. This result can be compared with the dispersion relation for noninteracting bosons in a spherically symmetric trap (2.9) which is (after subtracting the ground state energy)

$$\omega_{cl}(n_r, l) = \omega(2n_r + l) \quad (7.25)$$

The modes with no radial nodes ($n_r = 0$) are called the **surface excitations** for which (7.23) predicts the dispersion law

$$\omega_{cl} = \sqrt{l} \omega \quad (7.26)$$

. The frequency of these modes is smaller than the harmonic oscillator result $l\omega$ (2.9) except for the case of $l = 1$ mode (dipole mode, for details see [26]). At very low energy only these modes are excited. Therefore when the condensate is rotated, initially all the angular momentum are carried by these modes. Their time evolution under rotation actually determines how angular momentum is transferred from the surface to the bulk of the systems and leads to the nucleation of a vortex. Specially the surface mode with $l = 2$ and energy $\sqrt{2}\omega$, known as the quadrupole mode, plays a very prominent role in the vortex nucleation mechanism. Experimental traps are generally non-spherical but has an axis of symmetry. So we identify such surface modes in this geometry in the next section.

- Axisymmetric trap

In an axisymmetric confinement (§IIC) Eq. (7.21) writes as

$$\omega_{cl}^2 \delta\rho = \omega_\perp^2 \left(r \frac{\partial}{\partial r} + \lambda_R^2 z \frac{\partial}{\partial z} \right) \delta\rho - \frac{\omega_\perp^2}{2} (R_\perp^2 - r^2 - \lambda_R^2 z^2) \nabla^2 \delta\rho \quad (7.27)$$

where λ_R is the aspect ratio and $R_x = R_y = (1/\lambda_R)R_z = R_\perp$. Unlike the case of a spherical trap here all density fluctuation modes and their dispersion cannot be written in an analytic form. However, using the symmetry about the z -axis some specific low lying modes can be studied. Because of this symmetry the normal modes of density fluctuations are eigenmodes of the operator $L_z = \frac{\hbar}{i} \frac{\partial}{\partial \theta}$. We use θ as polar angle in the spherical polar co-ordinate system and as azimuthal angle in the cylindrical polar co-ordinate system. Also for notational convenience here we denote $l_z = \pm p$ where $p \in \mathbf{N}$. One class of such solutions is of the form

$$\delta\rho \propto z^p = (x + iy)^p = r^p Y_{p,\pm p}(\theta, \phi) \quad (7.28)$$

which have the dispersion

$$\omega_{cl}^2 = p\omega^2 \quad (7.29)$$

Therefore they can be identified as the surface modes. Similarly it can be verified that there are solutions of the form

$$\delta\rho \propto z(x + iy)^{p-1} = r^p Y_{p,\pm(p-1)} \quad (7.30)$$

with the frequencies given by

$$\omega_{cl}^2 = (p-1)\omega_{\perp}^2 + \omega_z^2 \quad (7.31)$$

These two modes are degenerate for a spherical trap and both of them surface modes.

To identify the quadrupole modes we note that for $\lambda_R \neq 1$, there is no spherical symmetry and as a result l is not a good quantum number. Since l determines the polarity, determining polarity of a general mode in this trap is difficult. But as shown in (7.28) and (7.30) there are eigenmodes in such a system which can be mapped on to the eigenmodes of the condensate in a spherically symmetric confinement and their polarity can be subsequently identified. In this way one gets following two expressions for the quadrupole density modulation from (7.28) and (7.30) [50] after setting $p = 2$, namely

$$\delta\rho \propto r^2 e^{\pm 2i\theta} = (x + iy)^2, \quad l_z = \pm 2 \quad (7.32)$$

$$\delta\rho \propto rze^{\pm i\theta} = z(x + iy), \quad l_z = \pm 1 \quad (7.33)$$

with their frequencies given by (7.29) and (7.31). Let us consider a linear combination of the two modes described in (7.32) of the form

$$\delta\rho \propto (x^2 - y^2) \quad (7.34)$$

Since this mode is a superposition of two eigenmodes with equal and opposite l_z , its angular momentum about the axis of symmetry is zero. If such a mode becomes the steady state solution of the system, using (7.5) it can be shown that the associated quadrupolar velocity field \mathbf{v}_s is given as $\propto \nabla(xy)$. Since the angular momentum about the z -axis is 0, such a field does not contain any vorticity. However if the trap is rotated new situation arises [58]. We discuss this in a later section.

E. Quadrupole modes in the presence of a vortex

In the earlier section it has been pointed out that if the confinement is isotropic in the x - y plane, two quadrupole modes having angular momentum $\pm l_z$ are energetically degenerate. Though this is true for a condensate without vortices, in the presence of a vortex this degeneracy is lifted [27, 47]. This can be explained by noting that the average velocity flow associated with the collective oscillation can be either parallel or opposite to the vortex flow, depending on the sign of the angular momentum carried by the excitation. This provides a chance to spectroscopically detect the presence of a vortex in the condensate. To that purpose Zambelli and Stringari [50], using a sum rule based approach, derived analytical expression which relates the splitting between the quadrupole modes with the average angular momentum per particle. For the details of the sum-rule approach see [65] and how this is applied to study the response of the quadrupole mode is given in detail in [50]. We shall just mention the expression obtained by Zambelli and Stringari which relates how the frequency difference between two quadrupole modes with equal and opposite angular momentum l_z is associated with the average angular momentum per particle in the superfluid. Within the sum-rule approach the splitting between the two frequencies can be written as

$$\omega_{+2} - \omega_{-2} = \frac{2}{m} \frac{\langle L_z \rangle}{\langle r_{\perp}^2 \rangle} = \frac{7\omega_{\perp}\kappa}{\lambda_R^{2/5}} \left(15 \frac{N_0 a}{a_{\perp}} \right)^{-2/5} \quad (7.35)$$

where ω_{+2} and ω_{-2} correspond to two quadrupole modes with $l_z = \pm 2$ and $a_{\perp} = \sqrt{\frac{\hbar}{m\omega_{\perp}}}$. This result has been subsequently used by the ENS [12] and JILA [9] group to measure the angular momentum of the condensate in the presence of a vortex.

VIII. EXPERIMENTS ON VORTICES IN BEC

In this section we describe the experiments done to detect the vortices and to study their properties in the atomic BEC. We also compare the results of these experiments with the theoretical predictions which have been described in the earlier sections.

The first experimental observation of vortices in a trapped condensate took place in JILA [8]. The experimental scheme is guided by a theoretical model proposed by Williams and Holland [66] which exploits the possibility of trapping otherwise identical (bosonic) atoms in

two different internal (hyperfine) states (chapter 3 of [4]). The basic idea [66] is as follows. Let us assume that identical atoms in two hyperfine states are trapped in two identical axially symmetric harmonic oscillator potentials, whose centers are spatially separated by a given distance. These two traps are rotated about the common axis of symmetry which passes through the center of the line joining the centers of these traps, with a frequency Ω . Simultaneously an electromagnetic field is applied that couples the two internal atomic hyperfine states. The coupling is parametrized by two parameters, namely the detuning δ_{dt} and the Rabi frequency \mathcal{R} . The detuning δ_{dt} gives the mismatch of the frequency of the coupling electromagnetic field to the frequency (energy) difference between the two hyperfine states. And \mathcal{R} gives the rate at which the population would oscillate between these two states if $\delta_{dt} = 0$.

The condensate wavefunction of this two-component BEC can be written as a two-component spinor. The symmetry of such wavefunction is different from that of a single-component BEC wavefunction [18]. For explaining the basic idea behind the vortex nucleation in this scheme, it is enough to consider the following part of the free energy functional in the co-rotating frame

$$F_{part}(rot) = \int d\mathbf{r} \sum_{i=1,2} \Psi_i^* (H_0 - \Omega L_z) \Psi_i + \frac{\hbar}{2} \delta_{td} (\Psi_1^* \Psi_1 - \Psi_2^* \Psi_2) \quad (8.1)$$

where 1 and 2 denotes two hyperfine states. We know that (§III F) the energy of a vortex with one unit of angular momentum ($\kappa = 1$) is shifted by $\hbar\Omega$ in the co-rotating frame relative to its energy in the laboratory frame. When this energy shift is compensated by the energy mismatch $\hbar\delta_{dt}$ due to detuning, one gets one condensate at rest in the center of the atomic cloud and the other in a unit vortex state around it. This has been realized in JILA [8]. Subsequently the central region can be removed and one gets a vortex state in a single-component BEC [67]. Apart from these experiments in JILA the other experiments to detect vortices is analogous to the Rotating Bucket experiment for the Superfluid ^4He [38]. In this experiment, at very low temperature the superfluid helium will come to the rest in the frame of a rotating bucket when the rotational frequency reaches a characteristic value. At this frequency a quantized vortex is nucleated in the superfluid. We discuss similar experiments done for the trapped condensate in the following section.

A. Rotating Bucket analogue for trapped atoms

For the trapped atom, the role of the bucket can be played by the trapping potential. Therefore a similar experimental set up may be constructed if one can rotate the trap in which the condensate is formed. Such an experimental set-up to detect vortices was first realized by the ENS group [10, 11] where the trap is put into rotation by stirring it with a laser beam. This leads to the observation of the vortex nucleation in the rotating trap. Subsequently employing the same technique MIT group [15, 16] also observed the nucleation of a large number of vortices. Vortices nucleated in this way arrange them in the form of a vortex lattice [68]. In the experiment done by the Oxford group [17] the trap is rotated by using magnetic fields instead of laser stirrer. Here we describe how the trap is rotated by using a stirring laser beam following [13].

B. Experimental realization of a rotating trap

The magnetic trap in which the BEC is confined is an axisymmetric harmonic potential:

$$V_{tr}(\mathbf{r}) = \frac{1}{2}m\omega_{\perp}^2(x^2 + y^2) + \frac{1}{2}m\omega_z^2z^2, \quad (8.2)$$

If the aspect ratio (2.13) $\lambda_R \ll 1$ the shape of the condensate is like a cigar with its height (TF radius in z -direction) is much larger than its diameter (TF radius in the transverse plane) [13, 15]. In the other limit ($\lambda_R \gg 1$) the condensate is like a pancake [9]. To create a rotating trap the condensate is stirred with a focused laser beam propagating along the symmetry axis (z -axis) of the trap and toggling back and forth very rapidly between two symmetric positions about the center of the trap. The electromagnetic field of the laser beam creates an average dipole potential in the $x - y$ plane which gives the following additional effective confinement

$$\delta V_{tr}(\mathbf{r}) = \frac{1}{2}m\omega_{\perp}^2(\epsilon_X X^2 + \epsilon_Y Y^2) \quad (8.3)$$

where X and Y are the co-ordinates in the co-rotating frame. This potential is rotated through an acousto-optic deflector which rotates the co-ordinates X and Y at an angular frequency Ω producing a rotating harmonic trap. Therefore

$$X = x \cos(\Omega t) + y \sin(\Omega t) \quad Y = -x \sin(\Omega t) + y \cos(\Omega t) \quad (8.4)$$

Defining $\omega_{X,Y}^2 = \omega_\perp^2(1 + \epsilon_{X,Y})$, the total confinement potential in the lab frame is given by

$$(V_{tr} + \delta V_{tr})(\mathbf{r}) = \frac{1}{2}m(\omega_X^2 X^2 + \omega_Y^2 Y^2) + \frac{1}{2}m\omega_z^2 z^2 \quad (8.5)$$

$$\begin{aligned} &= \frac{1}{2}m\bar{\omega}_\perp^2(x^2 + y^2) + \frac{1}{2}\lambda_R^2 m\omega_\perp^2 z^2 \\ &\quad + \frac{1}{2}m\epsilon\bar{\omega}_\perp^2((x^2 - y^2)\cos(2\Omega t) + 2xy\sin(2\Omega t)) \end{aligned} \quad (8.6)$$

with

$$\bar{\omega} = \sqrt{(\omega_X^2 + \omega_Y^2)/2} \quad \epsilon = (\omega_X^2 - \omega_Y^2)/(\omega_X^2 + \omega_Y^2) . \quad (8.7)$$

This potential is stationary in the rotating frame and oscillates periodically at frequency 2Ω in the laboratory frame (8.6). The stirring frequency Ω is chosen in the interval $(0, \omega_\perp)$ so that the condensate is stable. At the upper value of this interval, the centrifugal force equals the transverse restoring force of the trap. Similar technique to rotate the trap is employed in the MIT experiments with a varying range of intensity and frequency of the laser stirrer. Particularly the anisotropy ϵ in their trap is higher in comparison to the other experiments. The Oxford group [17] puts the atom in a combination of the spherical quadrupole magnetic field and a rapidly rotating bias field (magnetic). Together they form a time-averaged orbiting potential which is anisotropic in the transverse plane and also rotates the trap.

C. How to detect a vortex?

- **From the optical image of the condensate density**

In the rotating trap set-up the vortices will be nucleated when the stirring frequency exceeds a characteristic value Ω_{c1} . Usually the stirring frequency is equal to the frequency at which the trap is rotated. The TF density of the condensate with a vortex (6.4) vanishes at the center of the trap (vortex core). Therefore one may detect a vortex through the imaging of the density profile of the condensate. To this purpose the stirring potential is switched off adiabatically (in a time long compared to ω_\perp^{-1}) and the condensate density profile along the stirring axis is imaged to detect the presence of a vortex. The radius of the vortex core is of the order of the healing length (5.14) $\xi_0 = (8\pi\rho(0)a)^{-1/2}$ which is too small (like $\xi_0 \sim 0.2 \mu\text{m}$ in the experiments of the ENS group) to be observed optically in the experiments. To remove this difficulty the time of flight technique is used in which the trap is switched-off and the

condensate is allowed to expand for some time [71]. In this process the vortex core also gets expanded. The image of the enlarged condensate is then taken to detect the presence of a vortex.

- **Measurement of the angular momentum**

In the presence of a single vortex with winding number $\kappa = 1$ each particle in the superfluid carries on the average extra one unit (\hbar) of angular momentum. Therefore the presence of a vortex can be verified by measuring this extra angular momentum. Both ENS [12] and JILA [9] did this measurement to confirm the presence of a vortex in a rotating condensate. For this they used the result (7.35) obtained by Stringari and Zambelli [50] that in a cylindrically symmetric geometry in the presence of a vortex, the difference between frequencies of the two transverse quadrupole modes ω_{+2} and ω_{-2} , corresponding respectively to excitations with angular momentum $l_z = 2$ and $l_z = -2$ is proportional to the average angular momentum per particle (7.35). In a static condensate these two modes are degenerate. In the experiment [12] the condensate is subjected to the dipole potential created by stirring laser beam but with a fixed basis ($\Omega = 0$ in Eq. 8.4) such that $x = X$ and $y = Y$. Therefore one just have an elliptically deformed trap. This non-rotating dipole potential is applied for a period which is smaller than the quadrupolar oscillation period. The condensate is then allowed to oscillate freely in the pure magnetic trap. Using time-of-flight technique its image is then taken. This procedure was repeated in the presence as well as in the absence of a vortex. From the precessional frequency of the major and the minor axis of the ellipse the difference $\omega_{+2} - \omega_{-2}$ is determined. Using (7.35), the angular momentum per atom is measured from it.

D. Vortex nucleation in a deformed trap

In a static trap the confinement potential in the $x - y$ plane is isotropic. However once the rotation is switched on this is no more true since the stirring beam introduces an anisotropy in the confinement potential (§VIII B, Eq. 8.3). The anisotropy (8.7) can be set either suddenly [10, 15] or adiabatically [14, 17] resulting in an elliptic deformation of the condensate. This has important consequences for the process of vortex nucleation. ENS group [14] made a detailed study of the stationary state of the condensate when this

deformation is fixed at a given value and the rotational frequency is ramped up adiabatically. Their findings agree well with the theoretical prediction by Recati *et. al.*[58]. This stationary state becomes dynamically unstable beyond a characteristic rotational frequency. This leads to the nucleation of a vortex[59]. On the otherhand when the deformation is switched off suddenly the mechanism of vortex nucleation [59, 60] is different. We discuss this in a later section (§XI).

E. Rotating the normal cloud

In another experiment by the JILA group [9], instead of rotating the confining potential, the normal component of the atomic cloud which surrounds the superfluid atomic cloud is rotated while the trap stays at rest. To observe vortex nucleation in this set-up the non-condensate atoms which is in the normal state is rotated first and then they are cooled below the condensation temperature. As a result the superfluid fraction grows from zero to a finite value. However the boundary of the cloud is always formed of the normal-component and rotates like a rigid body. The superfluid part in the interior rotates only by creating a vortex. With increasing rotation the surface of the cloud gets inflated in the plane of rotation because of the centrifugal force. The rotational frequency can be measured from the change in the size of the cloud in the plane of the rotation using the following expression

$$\frac{\Omega}{\omega_{\perp}} = \sqrt{1 - \left(\frac{\lambda_R}{\lambda_R^0}\right)^2} \quad (8.8)$$

where λ_R^0 is the aspect ratio (2.13) of the static trap. The number of vortices in the superfluid is then determined from Ω .

F. How good experiments agree with the theory?

The comparison is done by comparing the theoretically determined (6.10) values of the characteristic frequency of the vortex nucleation [46, 47, 48] to the corresponding experimental results. The critical frequency of vortex nucleation is dependent on the several parameters such as the number of particles in the condensate, stirring mechanism, anisotropy in the trap potential, stirring time etc. Consequently the characteristic frequency in the vortex nucleation as a function of the transverse confinement frequency (ω_{\perp}) can vary in the

experiments. This ratio is ≈ 0.67 in [10] which is higher than the value calculated within TF approximation, ($\approx .41$) [46]. Moreover ENS experiments also do not show any strong dependence on the number of condensate particles which is also in contradiction to the TF prediction. For the parameters used in the MIT experiment [15] the theoretical (6.10) rotational frequency of the first vortex nucleation ($\approx 0.08\omega_{\perp}$) is also much smaller than the experimentally observed value ($\approx 0.3\omega_{\perp}$). In the JILA experiment [9], the characteristic frequency of vortex nucleation is given by $0.32\omega_{\perp} < \Omega_{c1} < 0.38\omega_{\perp}$ which is also higher than the TF estimation ($0.2\omega_{\perp} < \Omega_{c1} < 0.25\omega_{\perp}$). This is true also for the experiment done in Oxford [17]. Moreover according to the observations in ENS, MIT and Oxford the vortex nucleation in the BEC is always preceded by a strong deformation of the surface of the atomic cloud. Particularly in the experiments by the ENS [13] and the Oxford [17] group this deformation has been identified as a surface quadrupole mode. Experiments [14, 17] also point out mechanism of nucleation of a vortex is dependent on whether the trap is put into rotation adiabatically or suddenly. These experiments motivate a more local approach to study the process of vortex nucleation in a trapped BEC. Corresponding developments are discussed in subsequent sections.

IX. THE ROLE OF SURFACE BARRIER IN VORTEX NUCLEATION

We have seen in the last section that the thermodynamic frequency of the vortex nucleation determined within the TF approximation (6.10) is usually much smaller than the experimentally determined characteristic frequency of first vortex nucleation. This fact and the other experimentally observed features points out that the existence of the vortex state as a global minimum of the free energy of the condensate in the rotating frame beyond a certain characteristic rotation frequency is a necessary but not the sufficient criterion for the nucleation of a vortex. The presence of a vortex in the bulk of a condensate in a static axisymmetric trap is associated with an extra energy. Within the TF approximation it can be shown that this energy is highest when the vortex is centered at the center of the trap and decreases monotonically as a function of distance of the vortex center from the center of the trap [18, 60, 76]. Finally within TF approximation (without any boundary correction) this energy vanishes at the boundary of the system. The vortices are therefore nucleated from the surfaces. The dynamic evolution of the surface modes in a rotating trap and the

change in the energy landscape due to the presence of a vortex at a given distance from the center of the trap determines the mechanism of vortex nucleation in a trapped BEC. This will be discussed in the following sections. The discussion will start with the description of the Landau criterion of superfluidity [56], which when applied to the surface modes in a trapped condensate, determines at what rotational frequency such a mode will become energetically unstable towards the vortex nucleation in the center of a condensate.

A. Landau criterion of superfluidity

Landau criterion determines the condition for the superfluidity. Let us consider a particle of mass m' sent into the Bose-gas with an initial velocity \mathbf{v}_p . The particle can transfer energy and momentum to the Bose-gas only by creating an excitation of momentum $\hbar\mathbf{k}$ which causes viscous damping. If such an excitation is produced, with momentum $\hbar\mathbf{k}$, the momentum of the particle is reduced by the same amount $\hbar\mathbf{k}$. The conservation of energy therefore requires

$$E_{\mathbf{k}} = \frac{1}{2}m'\mathbf{v}_p^2 - \frac{1}{2m'}[m'\mathbf{v}_p - \hbar\mathbf{k}]^2 = \hbar\mathbf{k} \cdot \mathbf{v}_p - \frac{\hbar^2 k^2}{2m'}. \quad (9.1)$$

To produce a finite energy excitation, $|\mathbf{v}_p|$ has to satisfy the condition

$$|\mathbf{v}_p| \geq \left| \frac{\mathbf{k} \cdot \mathbf{v}_p}{k} \right| \geq \frac{E_{\mathbf{k}}}{k} \geq c_s. \quad (9.2)$$

The last expression follows from Bogoliubov dispersion law (4.10). This implies that a particle with an incoming velocity smaller than the sound velocity c_s can move through the condensate without causing any damping. Therefore there is no channel at very low temperature through which the interacting Bose gas can dissipate. This leads to its superfluidity. However, for an ideal Bose gas this condition gives

$$|\mathbf{v}_p| \geq \frac{E_{\mathbf{k}}}{k} \geq \frac{\hbar^2 k}{2m} \quad (9.3)$$

which makes it possible to excite an ideal Bose gas with an infinitesimal \mathbf{v}_p . Therefore it does not show superfluidity like a repulsively interacting Bose gas. Both systems however shows Bose-Einstein condensation.

We have already mentioned that for a trapped condensate the low energy excitations are the surface Bogoliubov modes (7.26) which has finite angular momentum. Therefore the

channel through which a trapped condensate can dissipate is these surface excitations. Dalfovo and Stringari [54] showed how the generalization of the Landau criterion can determine at what rotational frequency such a surface modes can be excited to nucleate a vortex in the condensate. Let us denote the frequency of such a surface mode as $\omega_s(l)$. Then the rotational frequency at which the l -th surface mode can be excited is given by

$$\Omega(l) = \frac{\omega_s(l)}{l} \quad (9.4)$$

This excited surface mode overcomes a potential barrier in the surface and get in the bulk in the form of vortex. The minimum of the rotational frequency determined in this way (9.4) therefore gives the characteristic frequency of first vortex nucleation, namely Ω_{c1} .

Within classical hydrodynamical approximation (7.26), the quantity $\frac{\omega_{cl}(l)}{l}$ monotonically decreases with increasing l and does not give a realistic value [54] for Ω_{c1} . This is because the classical hydrodynamic approximation (§VII B) is no more valid in the surface region where the kinetic energy is appreciable and the interaction energy is relatively weak. This problem was tackled in various ways. Dalfovo and Stringari used [54] a sum-rule based approach which fixes the upper limit of the frequency $\omega_s(l)$. Khawaja *et. al.*[53] modified the classical hydrodynamic approximation by including the surface correction to the TF density [51] and obtain the dispersion law for various surface width. Their treatment was subsequently improved by Anglin [55] through the use of a combination of analytical and numerical techniques and the determined critical frequency from the Landau criterion agrees well with the MIT experiment [15]. Simula *et. al.*[32] obtained the surface dispersion relation by numerically solving Bogoliubov equations in a rotating frame. Here we provide a brief discussion on the role of surface excitations in the vortex nucleation process.

B. The order-parameter at the surface of the cloud

To find out the dispersion relation of the surface modes one needs to take into account the modification of the TF approximation (§V A) near the surface of a condensate. This was carried out by Dalfovo *et. al.* [51]. They started by identifying the characteristic length scale over which the condensate wavefunction at the surface goes to zero, namely the healing length (3.16) at the surface. To that purpose one starts with a spherical trap of radius R such that $\mu_{TF} = V_{tr}(R)$ (5.8). Then by doing a Taylor expansion of $V_{tr}(r)$ about the point

R when $|R - r| = \Delta \ll R$, one obtains

$$V_{tr}(r) = \mu_{TF} - |\nabla V||_{r=R}\Delta + o(2) \quad (9.5)$$

where the derivative is taken along the direction perpendicular to the surface at $r = R$. F is the modulus of the attractive external force such that $\mathbf{F} = -\nabla V_{tr}$ evaluated at $r = R$. Therefore, near the surface the confinement potential takes the form of a linear ramp potential. Close to the boundary, where $|r - R| \ll R$, the GP equation (3.10) takes the form

$$-\frac{\hbar^2}{2m} \frac{d^2}{dr^2} \Psi + (r - R)F\Psi + g\Psi^3 = 0. \quad (9.6)$$

Comparing this equation with the one obtained under the usual TF approximation (5.6) we see that the difference comes from the inclusion of the term due to the kinetic energy (only the most dominant contribution is taken) as well as the change in the form of the confinement potential. The surface healing length can now be determined as

$$\delta_s = \left(\frac{2m}{\hbar^2} F \right)^{1/3} \quad (9.7)$$

Using this length scale as the unit of the length and scaling the wavefunction Ψ by $\delta_s(8\pi a)^{1/2}$ the equation (9.6) can be written in a dimensionless form giving

$$\overline{\Psi}'' - (x + \overline{\Psi}^2)\overline{\Psi} = 0. \quad (9.8)$$

Here $\overline{\Psi} = \delta_s(8\pi a)^{1/2}\Psi$ and $x = \frac{r-R}{\delta_s}$. The above equation can be solved to give the surface wavefunction and the solutions are given in [51]. We mention here the asymptotic form which gives an exponentially vanishing tail for the condensate wavefunction

$$\overline{\Psi}(x \rightarrow \infty) \simeq \frac{A_1}{2x^{1/4}} \exp\left(-\frac{2}{3}x^{3/2}\right) \quad (9.9)$$

The Thomas-Fermi solution of Ψ and the solution of (9.8) determine the behavior of the wave function in two distinct regions of space: the former in the interior of the cloud, the latter in the boundary region. A full description of the condensate wavefunction is obtained by matching these two-type of solutions. The correction to the TF approximation is then extended to the hydrodynamic theory to obtain the dispersion relation of the surface modes. This will be discussed now.

C. Surface modes from the hydrodynamic theory

The harmonic potential can be approximated as a linear ramp potential in the surface region (9.6). Therefore, one can reformulate the classical hydrodynamic equation for the collective excitations (7.21) in the surface of the condensate by replacing the harmonic confinement with this linear ramp potential [53] (also see chapter 7 of [4]). To study the surface modes one introduces a local two-dimensional co-ordinate system in the surface. The x axis of this local co-ordinate system is then identified with the direction of the gradient of this linear ramp potential. Along the other direction there is no such force and hence $\delta\rho$ in this direction can be chosen as plane wave. We use δ_s (9.7) as the unit of length and $\tau = (\frac{2m\hbar}{F^2})^{1/3}$ as the unit of time. Then the equilibrium density (9.8) has the form $\rho = |\bar{\Psi}|^2 = -x$ for $x < 0$ and 0 for $x > 0$ (neglecting the derivative). To obtain the surface dispersion relation one looks for the following type of the solutions

$$\delta\rho = f(qx)e^{qx+iqz} \quad (9.10)$$

The equation (7.21) gives the dispersion relation as

$$\omega_s^2 = 2q(1 + 2n), n = 0, 1, 2, \dots \quad (9.11)$$

$$\delta\rho(x, z, t) = C_n L_n(-2qx)e^{qx+iqz-i\omega t} \quad (9.12)$$

where $L_n(-2qx)$ is the Laguerre polynomial and C_n is a constant. Following [53] we shall now state the conditions under which this dispersion law for the surface modes becomes same with the one determined (§VII D) under the global hydrodynamic approximation. For l much greater than n , the dispersion relation (7.23) becomes $\omega_{cl}^2 = \omega^2 l(1+2n)$. The spherical cloud density has the l dependence of the form $P_l^m(\cos\theta)$ which has the same periodicity of $\cos(l\theta)$ (or $\sin(l\theta)$). The wave number q on the surface of this cloud is therefore given by

$$q = \frac{2\pi}{\lambda_q} = \frac{1}{R} \frac{2\pi R}{\lambda_q} = \frac{l}{R} \quad (9.13)$$

At the boundary the restoring force is $F = m\omega^2 R$ (gradient of the harmonic potential) Eliminating R therefore one gets the agreement $\omega_{cl}^2 = \omega^2 l(1+2n) = 2q(1+2n) = \omega_s^2$ (again in the dimensionless unit). For $l \gg n$ it is therefore a good approximation to replace the parabolic confinement with a linear ramp potential. The reason is that the characteristic

penetration depth for a mode is of the order $\frac{2n+1}{q} = \frac{(2n+1)R}{l}$ from the surface. For $n \ll l$ this is much smaller than R and the assumption that these modes are confined in the surface region is then satisfied. The agreement is however true for all l when $n = 0$ in the relation (7.23).

In the above derivation only the change in the form of the confinement potential from harmonic to linear ramp is taken into account. But the correction due to the surface kinetic energy ($\bar{\Psi}''$ in Eq.9.8) which gives a non vanishing quantum pressure (7.12) term in the hydrodynamic equation is neglected. However when the healing length δ_s (9.7) is not negligible compared to the wavelength of the surface modes this term is no more negligible. Incorporating the corrections coming from the non-vanishing surface kinetic energy through a variational approach Khawaja *et. al.* [53] obtained the following dispersion relation (again in the dimensionless unit and for lowest n)

$$\omega_s^2 \equiv 2q + 4q^4[-\log q + 0.15] \quad (9.14)$$

This observation agrees with the results by Fetter and Feder [52] where they have considered the corrections to the Thomas-Fermi description of the condensate due to the presence of the boundary layer near the condensate surface.

Anglin [55] extended this analysis of surface modes with small wave-vector q by going beyond Bogoliubov approximation through a combination of numerical and analytical techniques. For $0 \leq q \leq 2$ the dispersion relation (in dimensionless form) turns out to be

$$\omega_s^2 = 2q + 1.35q^3 + 0.711q^4 \quad (9.15)$$

Then the ratio $\frac{\omega_s(q)}{q}$ is minimized to give the characteristic rotational frequency of the first vortex nucleation. The critical frequency determines in this way agrees very well with the experimentally observed value in MIT[15] where a strong deformation due to the stirring laser beams can excite a surface modes of very large l and the deformed surface region has a non-negligible width. For the parameters of MIT experiment using (9.13) Anglin has found that the mode with $l = 18$ is unstable against the vortex formation when the rotational frequency $\Omega \sim 0.3\omega_\perp$ in an axisymmetric trap. The agreement is however not so good for the other experiments [9, 10, 14, 17]. Particularly for the experiment in JILA [9] where the normal cloud is rotated in a static trap, vortices are nucleated before a surface mode is excited. For a more detailed discussion on the conditions under which the determination

of the critical frequency based on Landau criterion works well, we refer to [54] and [55]. In a later chapter we shall discuss a different theoretical framework to understand the vortex nucleation from the surface which is particularly relevant to the experiments [10, 14, 17]. Before that we shall discuss how the process of vortex nucleation can be studied by applying a set of non-local and chiral boundary conditions to the linear Schrödinger equation.

X. ROLE OF BOUNDARY CONDITIONS IN NUCLEATING VORTICES

In the earlier sections we have discussed the process of vortex nucleation in the framework of repulsively interacting bosons using various approximations. In this section we shall provide an alternative description of this process where the effect of the interaction can be replaced by a set of non-local and chiral boundary conditions applied to an otherwise non-interacting problem. To determine the condensate wavefunction $\Psi(\mathbf{r})$ in a confined geometry like that of trapped condensate, one has to impose boundary conditions. The GP equation (3.10) is equivalent to a single boson problem in an effective one body potential V_E , given by

$$V_E = V_{tr} + g|\Psi(\mathbf{r})|^2 \quad (10.16)$$

Because of the presence of the non-linear term $g|\Psi(\mathbf{r})|^2$, this equation has to be solved self-consistently with a suitable boundary condition [72]. The problem becomes much simpler if there is a way to replace the non-linear term by a suitable choice of the boundary conditions. Generally such a replacement is difficult. This is because there is no known mapping available between the boundary conditions and the effective one body potential which they aim to replace ($g|\Psi(\mathbf{r})|^2$ in the present problem) except for some simple cases. Therefore the choice of boundary conditions depend on what type of effect generated by the effective one body potential the boundary condition is expected to simulate.

In the present case we aim to study the process of vortex nucleation in a confined geometry by solving the linear Schrödinger equation with a set of such boundary conditions. For simplicity we consider a strictly two-dimensional problem. The proposed boundary conditions are motivated by the following consideration. From the previous discussion we see that the dispersion law for surface excitations determines the characteristic rotational frequency of vortex nucleation. For a two-dimensional problem, equivalent of the surface states are the edge states. The proposed boundary condition therefore should be able to isolate these

edge states from the bulk states. The edge states should have higher angular momentum relative to the bulk states. If the proposed boundary conditions can ensure this then we want to see whether with the increasing rotational frequency it is energetically favourable for a state with higher angular momentum to be transferred from the edge to the bulk. This process can then be identified with the nucleation of a vortex. In the following section we shall describe a set of boundary conditions which satisfy these conditions. Details of this method is given elsewhere [57].

A. Chiral boundary conditions (CBC)

We consider the problem of a two-dimensional isotropic harmonic oscillator in a co-rotating frame rotating with angular velocity Ω about the z -axis. This problem has already been discussed in the section §II C. There effectively the boundary conditions are put at infinity. Now we seek the solutions of the problem in a circular domain of radius R . The eigenfunctions and eigenvalues in an infinite domain are already given in (2.15) and (2.18) of section §II. Using (2.19) the current density can be derived for a given eigenstate

$$\mathbf{j} = \frac{\hbar}{2mi} (\Psi_{n,lz}^* \nabla \Psi_{n,lz} - \Psi_{n,lz} \nabla \Psi_{n,lz}^* - 2i \frac{m}{\hbar} \mathbf{A}_\Omega |\Psi_{n,lz}|^2) \quad (10.17)$$

We have here changed the notation from Φ_n to Ψ_n since they represent the condensate wavefunction and not a single boson wavefunction. The hamiltonian and the Schrödinger equation are however same as those in the single boson problem. With the type of eigenfunctions given in (2.15) it can be checked that the radial component of such a current density vanishes while its azimuthal component is given by

$$j_\theta = \frac{\hbar}{m} \left(\frac{l_z}{r} - \frac{m}{\hbar} \Omega r \right) |\Psi_{n,l}|^2 \quad (10.18)$$

We define $b_\Omega = \frac{m\Omega}{\hbar}$. This has the dimension of $\frac{1}{L^2}$ and is related to b_{ω_\perp} through $b_\Omega = \frac{\Omega}{\omega_\perp} b_{\omega_\perp}$. Then with each angular momentum quantum number one can associate a length defined as

$$r_{l_z} = \sqrt{\frac{l_z}{b_\Omega}} \quad (10.19)$$

For $r < r_{l_z}$, j_θ is positive and for $r > r_{l_z}$ it is negative while it vanishes at $r = r_{l_z}$. Using the fact that the hamiltonian (2.19) is same as that of a charged particle in an effective magnetic field $2\Omega\hat{z}$ we call the currents in these two regions respectively paramagnetic and

diamagnetic. For a domain of radius R we also defined quantities those are similar to the magnetic flux in the corresponding Landau problem. In a dimensionless form they are given by

$$\Phi_\Omega = b_\Omega R^2, \quad \Phi = b_{\omega_\perp} R^2 \quad (10.20)$$

Now let us define the bulk and the edge regions using this particular value of r_{l_z} as a reference for a given angular momentum state such that the current associated to that particular angular momentum is respectively paramagnetic and diamagnetic in the bulk and the edge. Alternatively, one can define the bulk and the edge states for a disc of size R . The bulk states will have angular momentum $l_z < b_\Omega R^2$ whereas the edge states have $l_z \geq b_\Omega R^2$. We propose a set of non-local and chiral boundary conditions for the present problem which split the Hilbert space into a direct sum of two orthogonal, *infinite dimensional* spaces corresponding to bulk and edge states which respectively have positive and negative chirality on the boundary. The chirality is determined by the direction of the azimuthal velocity projected on the boundary. The azimuthal velocity $\frac{j_\theta(r)}{|\psi(r)|^2}$ projected on the boundary of the disc has eigenvalues given by

$$\lambda(R) = \frac{1}{R}(l_z - b_\Omega R^2) = \frac{1}{R}(l_z - \Phi_\Omega) \quad (10.21)$$

The chiral boundary conditions are defined in the following way:

1. For $\lambda \geq 0$, namely for $0 < \Phi_\Omega \leq l_z$,

$$\partial_r \Psi_{l_z}|_R = 0 \quad (10.22)$$

This holds for any n and henceforth we shall drop the subscript n in Ψ .

2. For $\lambda < 0$, namely for $l_z < \Phi_\Omega$,

$$(\frac{\partial}{\partial r} + \frac{i\partial}{r\partial\theta} + b_\Omega r)\Psi_{l_z}|_{r=R} = 0 \quad (10.23)$$

For the first set of wavefunctions which accounts for the edge states we use Neumann boundary conditions. We could have used as well Dirichlet boundary conditions. However unlike Neumann boundary conditions they give an unphysical discontinuity [73, 74]. These wavefunctions are more and more localized towards the outer side of the system with increasing rotational frequency. For states with $l_z < \Phi_\Omega$, whose wavefunctions are localized well inside

the disc, we impose the mixed boundary conditions (10.23). These boundary conditions are akin to the boundary conditions introduced by Atiyah, Patodi and Singer (APS) in their studies of Index theorems for Dirac operators with boundaries [75]. Similar boundary conditions have also been applied to the Landau problem on manifolds with boundaries [73, 74].

B. Spectrum with CBC and the vortex nucleation

To describe the spectrum let us introduce the dimensionless form of the energy, namely

$$\varepsilon = \frac{2mE_{n,l_z}R^2}{\hbar^2} = \left(\frac{2E_{n,l_z}}{\hbar\omega_{\perp}}\right)\Phi \quad (10.24)$$

where Φ is defined in (10.20). According to the chiral boundary conditions when Φ is increased at a fixed $\frac{\Omega}{\omega_{\perp}}$, the sign of the eigenvalues $\lambda(R)$ changes from positive to negative. Correspondingly the energy ε (10.24) of a state with a given n and l_z changes. This change in energy describes the corresponding transfer of a state from the edge to the bulk Hilbert spaces at the point $\Phi_{\Omega} = l_z$ (10.22-10.23). as shown in Fig.1. For large Φ , the infinite plane solutions (2.16) are reached asymptotically.

C. Spectrum with CBC

For an infinite system we have $\frac{\varepsilon}{4\Phi} = n + \frac{1}{2}(1 + (1 - \frac{\Omega}{\omega_{\perp}})l_z)$. Therefore $\frac{\varepsilon}{4\Phi}$, for a given $\frac{\Omega}{\omega_{\perp}}$, is a linear function of l with slope $(1 - \frac{\Omega}{\omega_{\perp}})$. When chiral boundary conditions are applied, this behaviour is approximately obeyed for the bulk states. But for the edge states the energy increases non-linearly with increasing angular momentum.

The Fig.2 shows the effect of an increase of the rotational frequency on the spectrum under the choice of CBC. We have plotted the energies of the bulk and the edge states for four different values of $\frac{\Omega}{\omega_{\perp}}$. For each value of $\frac{\Omega}{\omega_{\perp}}$, the quantity Φ_{Ω} is increased by unit steps from 1 to 3 and the corresponding bulk and edge energies are shown. Under these conditions, the slope of the bulk energy levels increases while the slope of the edge energy levels goes down. The opposite behaviour is observed when, for a fixed Φ_{Ω} , the ratio $\frac{\Omega}{\omega_{\perp}}$ increases. There are therefore certain values of the ratio $\frac{\Omega}{\omega_{\perp}}(< 1)$, at which the edge states for a given $\Phi_{\Omega} = l_z$ just intersect the bulk state corresponding to $\Phi_{\Omega} = l_z + 1$. The first

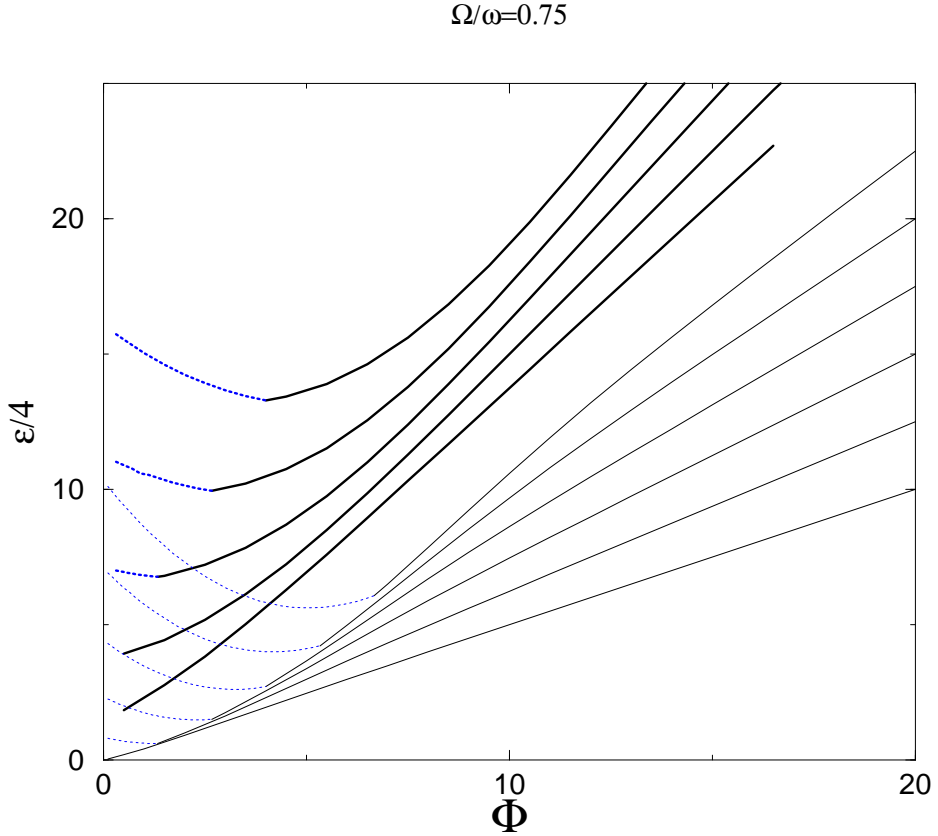


FIG. 1: *Energy levels with chiral boundary condition.* Energy levels for the first few angular momentum states are shown for $n = 0$ and $n = 1$. Each curve corresponds to a given value of the angular momentum. They correspond to $n = 0$ and l_z between 0 and 5 (thin lines for bulk states and thin dotted lines for edge states) as well as $n = 1$ and l_z between -1 and 3 with $l_z = -1$ corresponds to the lowest curve (thick lines for bulk states and thick dotted lines for the edge states). For $l_z > 0$ the spectrum has a kink at the point $l_z = \Phi_\Omega = \frac{\Omega}{\omega_\perp} \Phi$.

vortex is nucleated for $l_z = 1$. The characteristic rotational frequency is denoted by Ω_{c1} . The rotational frequency at which the edge states for $\Phi_\Omega = 1$ intersects the bulk states of the i -th vortex with $l_z = 1$ is denoted by Ω_{ci} .

A finite Bose-Einstein condensate without any vortex is defined when the domain of radius R (bulk region) contains only the state $l_z = 0$ such that $R = r_1$ (10.19). The boundary is given by $\Phi_\Omega = 1$ and the corresponding bulk and edge energy levels are shown as a function

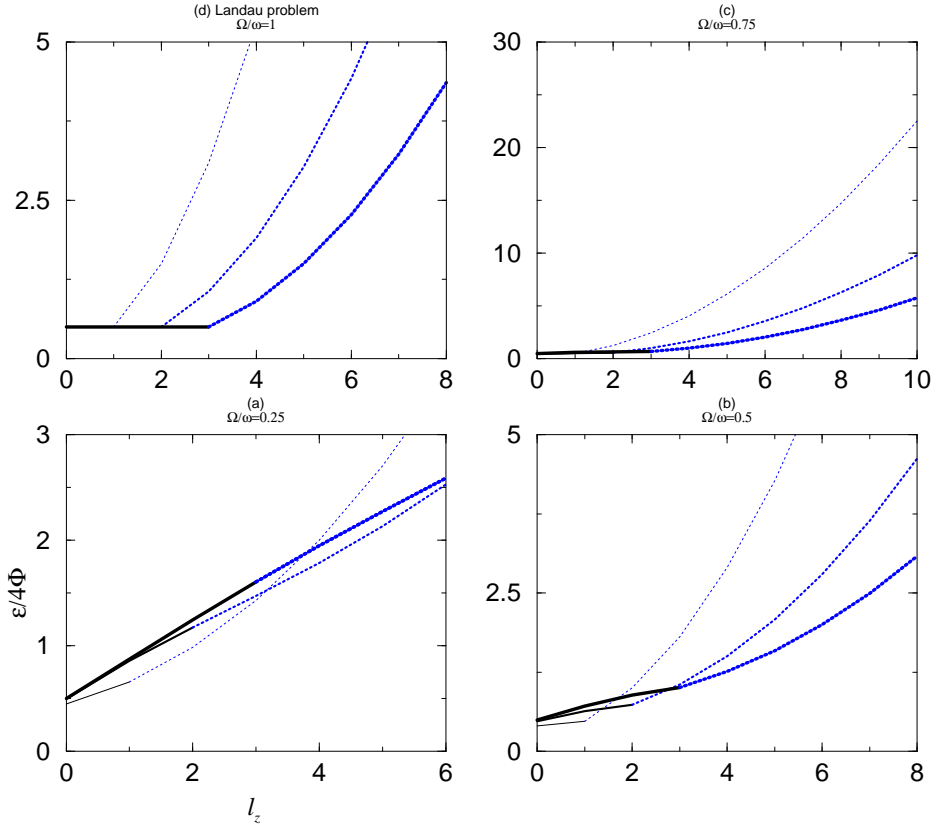


FIG. 2: *Effect of a faster rotation.* In these figures we have plotted $\frac{\varepsilon}{4\Phi}$ as function of l_z for a set of $\frac{\Omega}{\omega_\perp}$ values (given above each figure). The three set of plots in each figure correspond to $\Phi_\Omega = 1, 2, 3$ (the thinnest one for $\Phi_\Omega = 1$ and the thickest one for $\Phi_\Omega = 3$). The dotted part corresponds to edge states while the continuous part corresponds to bulk states. For $\frac{\Omega}{\omega_\perp} = 1$ bulk states for all three values of Φ_Ω fall on the same line.

of the ratio $\frac{\Omega}{\omega_\perp}$ in the Fig.2. When $\Phi_\Omega = 2$ instead for $\Phi_\Omega = 1$, the state with $l_z = 1$ is transferred from the edge to the bulk Hilbert space. For $\Omega \geq \Omega_{c1}$ the energy $\frac{\varepsilon}{4\Phi}(l_z)$ (10.24) of any state with $l_z \geq 2$ is less if $\Phi_\Omega = 2$ instead of $\Phi_\Omega = 1$. At $\Omega = \Omega_{c1}$ the boundary is given by $\Phi_\Omega = 2$. The state with $l_z = 1$ is now transferred to the bulk Hilbert space at this characteristic frequency. The bulk region has now one unit($\frac{h}{m}$) of extra rotational flux. Thus for $\Omega = \Omega_{c1}$ a vortex with $\kappa = 1$ is nucleated in the bulk. At this characteristic value for Ω the region with $R = r_2$ (10.19) is defined as a condensate with a single vortex of $l = 1$.

From these boundary conditions we can thus determine the characteristic frequency of

nucleation of the first vortex in terms of the trap frequency. It lies in between $\Omega = 0.35\omega_{\perp}$ and $\Omega = 0.36\omega_{\perp}$. We note that this characteristic frequency of nucleation is close to the value $\Omega = 0.29\omega_{\perp}$ that has been observed in one of the experiments [15] where ω_{\perp} is the trap frequency in the transverse direction.

D. Vortex nucleation at $\Omega > \Omega_{c1}$

We have so far discussed only the the nucleation of the first vortex with $\kappa = 1$ and we have determined the characteristic rotational frequency. With a further increase of the rotational frequency the boundary is successively given by $\Phi_{\Omega} = 3, 4, 5, \dots$. Correspondingly more than one higher angular momentum states are transferred from the edge to the bulk Hilbert space at a time. The characteristic rotational frequencies are respectively given by $0.42 < \frac{\Omega_{c2}}{\omega_{\perp}} < 0.43$, $0.46 < \frac{\Omega_{c3}}{\omega_{\perp}} < 0.47$, $0.48 < \frac{\Omega_{c4}}{\omega_{\perp}} < 0.49$. For example, if the rotational frequency of the trap is ramped up to Ω_{c2} and the system is allowed to come to equilibrium in the co-rotating frame, the boundary is given by $\Phi_{\Omega} = 3$ instead of $\Phi_{\Omega} = 1$. Since this is accompanied by the transfer of two units of the rotational flux quanta to the bulk, either two vortices each with $\kappa = 1$ are nucleated or a single vortex with $\kappa = 2$ is nucleated. The first of these two alternative situations implies that at $\Omega = \Omega_{ci}$, i number of vortices with $\kappa = 1$ enters. Alternatively the rotational frequency may be increased adiabatically from 0 to a higher value. The first vortex will enter at Ω_{c1} . The second vortex with $\kappa = 1$ enters when the bulk states for $\Phi_{\Omega} = 3$ just intersects edge states for $\Phi_{\Omega} = 2$. The corresponding rotational frequency is relatively higher.

Some features of the vortex nucleation can thus be explained by replacing the non-linear interaction with the chiral boundary conditions. Quantitative comparison of the theory with experimental predictions is difficult since the experimental geometry is generally more complicated than a pure two-dimensional disk. Particularly we have not considered the deformation of the the trap from the initial circular shape in the plane of the rotation [10, 14, 15, 17]. This deformation effects the process of the vortex nucleation in these rotating traps. In the following section we shall briefly describe how this deformation is incorporated in the theoretical description of the problem of vortex nucleation.

XI. VORTEX NUCLEATION IN A DEFORMED TRAP

It is mentioned in section §VIIID that to rotate the trap an anisotropy (8.7) is introduced in the confinement potential by a laser stirrer. This stirrer is then rotated to create the rotating harmonic trap. Subsequently, beyond a characteristic rotational frequency the first vortex is nucleated. In this section we discuss the role of this anisotropy in the vortex nucleation. To that purpose, following [58] we start by considering the steady state solutions of the hydrodynamic equations (7.15-7.16) in such rotating traps.

A. Stationary states in the rotating frame

It is already known from classical hydrodynamics that for a uniform fluid in a rotating elliptical cylinder, the instantaneous induced velocity field in the lab frame is given by [18, 69]

$$\mathbf{v}_{cl} = \Omega \frac{A^2 - B^2}{A^2 + B^2} \nabla(xy) \quad (11.25)$$

where A and B are the major and the minor axis of the ellipse. In order to solve the equations (7.15-7.16) one may therefore propose an ansatz velocity field of the following form

$$\mathbf{v}_s \propto \alpha \nabla(xy) \quad (11.26)$$

Here x and y are now the co-ordinates in the co-rotating frame (identical as X and Y in §VIIID). The corresponding steady-state ellipsoidal density can be written in the usual TF form (5.10)

$$\rho(\mathbf{r}) = \frac{1}{g} \left[\mu_{TF} - \frac{m}{2} (\tilde{\omega}_x^2 x^2 + \tilde{\omega}_y^2 y^2 + \omega_z^2 z^2) \right] \quad (11.27)$$

with

$$\begin{aligned} \tilde{\omega}_x^2 &= \omega_x^2 + \alpha^2 - 2\alpha\Omega \\ \tilde{\omega}_y^2 &= \omega_y^2 + \alpha^2 + 2\alpha\Omega \end{aligned} \quad (11.28)$$

To see why the above form of the steady state density corresponds to a quadrupole mode let us rewrite it as

$$\rho(\mathbf{r}) = \frac{1}{g} \left[\mu_{TF} - \frac{m}{2} ((\omega_\perp^2 + \alpha^2)r^2 + \omega_z^2 z^2) \right] - \frac{1}{g} \left[\frac{m}{2} (\epsilon - 2\alpha\Omega)(x^2 - y^2) \right] \quad (11.29)$$

In terms of the co-ordinates in the co-rotating frame, the steady state density is therefore a sum of the usual TF density in a static trap (after replacing ω_{\perp}^2 with $\omega_{\perp}^2 + \alpha^2$) and a quadrupolar density. The deformation of the trap is given by a quantity δ such that

$$\delta = \frac{\tilde{\omega}_x^2 - \tilde{\omega}_y^2}{\tilde{\omega}_x^2 + \tilde{\omega}_y^2} = \frac{\epsilon - 2\alpha\Omega}{1 + \alpha^2} \quad (11.30)$$

The continuity equation (7.15) requires that

$$\alpha = -\delta\Omega \quad (11.31)$$

These equations are satisfied simultaneously provided

$$\alpha^2 + \alpha(\omega_{\perp}^2 - 2\Omega^2) + \Omega\epsilon\omega_{\perp}^2 = 0 \quad (11.32)$$

Solution of the above equation gives the stationary solutions in the Ω, α plane and has been analyzed in detail in [58]. We mention some special features. For a symmetric trap potential ($\epsilon = 0$) if $\Omega < \frac{\omega_{\perp}}{\sqrt{2}}$, $\alpha = 0$. Substituting this in (11.29) gives the usual TF density of the cloud in an axisymmetric trap (5.10). However for $\Omega < \frac{\omega_{\perp}}{\sqrt{2}}$, the equation gets a new class of solutions which correspond to $\alpha = \pm\sqrt{2\Omega^2 - \omega_{\perp}^2}$. This non-zero value of α for $\epsilon = 0$ corresponds to a spontaneous deformation of the cloud to a quadrupolar shape. The physical origin of this spontaneous deformation of the trap is as follows. With the increase in the rotational frequency the energy of the quadrupolar state with $l_z = +2$ monotonically decreases to 0 till $\Omega = \omega_{\perp}$. Beyond this value of Ω the energy of this mode becomes negative. This leads to a thermodynamic instability and the system is spontaneously deformed at this Ω . For non-zero ϵ , the phase diagram corresponds to two branches of solutions known respectively as, the normal branch and the over-critical branch. We do not detail these results any further and now go to the issue of vortex nucleation in such a deformed trap.

B. Adiabatic switch on of the rotation

The above mentioned solutions are stationary solutions of the hydrodynamic equations in the rotating frame. So, to produce them experimentally the rotation has to be ramped up adiabatically for a fixed anisotropy ϵ . In the corresponding experiments [13, 17] it is found that at higher rotational frequency which is generally around $\Omega = \frac{\omega_{\perp}}{\sqrt{2}}$, these stationary solutions show dynamic instability leading to the vortex nucleation. By performing a linear

stability analysis of the equations of rotational hydrodynamics Sinha and Castin [59] showed that this is indeed the case. They found that if ϵ is very close to 0, at $\Omega = \frac{\omega_{\perp}}{\sqrt{2}}$, a large quadrupole oscillation makes the stationary solution dynamically unstable. For larger ϵ the dynamic instability occurs over a larger range of Ω around $\Omega = \frac{\omega_{\perp}}{\sqrt{2}}$. Solving the time dependent GP equation (see also [77]) they also verified that this dynamic instability leads to the vortex nucleation. Their findings are particularly in agreement with the experimental results in [13].

C. Sudden switch on of the rotation

The early ENS experiments [10, 12] and the MIT experiments [15, 16] come under this class. Here the stirring potential is rotated at a fixed frequency Ω and the deformation (ellipticity) due to the stirrer is switched on suddenly to a given value of ϵ . In the MIT experiment [15] the deformation is large and consequently it excites high polarity surface modes. We have already discussed in (§IX C) how the characteristic nucleation frequency can be obtained in this case [55] by using the Landau criterion. However in the other experiments the deformation is relatively less and the vortex nucleation can be understood by studying the quadrupole modes. Here we discuss the vortex nucleation mechanism following Kraemer *et. al.*[60]. Their study involves the evaluation of the energy of a displaced vortex [18, 44, 76] in the presence of a surface quadrupolar deformation under the sudden switch on of the trap deformation.

We start by evaluating the extra energy and the angular momentum associated with the presence of a straight vortex line with $\kappa = 1$ in a perfectly cylindrical axisymmetric trap (axis of symmetry is again the z -axis) displaced from the center of the cylinder by a distance d . The corresponding expressions in TF approximation are respectively

$$L_z(d/R_{\perp}) = N_0 \hbar \left[1 - \left(\frac{d}{R_{\perp}} \right)^2 \right]^{5/2}, \quad (11.33)$$

and

$$E_v(d/R_{\perp}, \mu_{TF}) = E_v(d = 0, \mu_{TF}) \left[1 - \left(\frac{d}{R_{\perp}} \right)^2 \right]^{3/2}, \quad (11.34)$$

where $E_v(d/R_{\perp}, \mu_{TF})$ is given in (6.8). According to (11.33) and (11.34) if the vortex is exactly located at the boundary it neither carries extra angular momentum nor energy

relative to a vortex free condensate. When the trap is rotated with angular velocity Ω about the z -axis the energy of the system in the co-rotating frame is given by

$$E_v(d/R_\perp, \Omega, \mu_{TF}) = E_v(d = 0, \mu_{TF}) \left[1 - \left(\frac{d}{R_\perp} \right)^2 \right]^{3/2} - \Omega N_0 \hbar \left[1 - \left(\frac{d}{R_\perp} \right)^2 \right]^{5/2}. \quad (11.35)$$

From this expression one finds that a vortex at $d = 0$ is energetically favorable if the rotational frequency satisfies $\Omega \geq \Omega_{c1}(\mu_{TF}) = E_v(d = 0, \mu_{TF})/N_0 \hbar$ which is the thermodynamic criterion of vortex stability (§III F). However, even for $\Omega \geq \Omega_v(\mu)$ and hence if $E_v(d/R_\perp, \Omega, \mu)$ is negative at $d = 0$, the energy exhibits a maximum at intermediate values of d that lies between 0 and R_\perp . Therefore if the rotation is suddenly switched on at a value greater than Ω_v , because of this energy barrier a vortex cannot be nucleated into the center of the trap though the vortex state is a global minima of the energy. To summarize the situation, the energy landscape will look like a valley representing this global minima surrounded by this energy barrier. As suggested by the experiments in ENS, MIT and Oxford, the disappearance of the barrier at sufficiently high angular velocity is preceded by a quadrupolar deformation of the atomic cloud. Therefore this energy landscape changes in the presence of a quadrupolar mode. In an elliptically deformed trap the energy of a quadrupole deformation in the rotating frame is given by [58]

$$E_Q(\delta, \frac{\Omega}{\omega_\perp}, \epsilon, \mu_{TF}) = N_0 \mu_{TF} \left[\left(\frac{2}{7} \right) \frac{1 - \epsilon \delta - (\frac{\Omega}{\omega_\perp})^2 \delta^2}{\sqrt{1 - \epsilon^2} \sqrt{1 - \delta^2}} + \frac{3}{7} \right]. \quad (11.36)$$

In [60] using this expressions the total energy of a quadrupole deformed condensate in presence of a displaced vortex can be evaluated. The energy landscapes are then redrawn at various values of the rotational frequency to understand the role of quadrupole deformation on the previously described energy barrier under sudden switch on of the deformation of the trap. At the time of the sudden switch-on of the deformation, $\delta = 0$. This corresponds to $\epsilon = 0$. Then the system will evolve through a set of intermediate configurations before attaining a stable value of the deformation parameter δ . By noting the corresponding changes in the energy barrier it is found [60] that at a given value for the trap deformation δ the a saddle is created in the energy barrier such that the vortex energy along that path continually decreases from the surface to the center. At this point the vortex nucleates. This explains the vortex nucleation mechanism under the sudden switch on of the trap deformation.

XII. CONCLUSION AND OUTLOOK

In this article we have discussed the problem of vortex nucleation in a finite quantum system, namely the trapped atomic condensate. We have described how the thermodynamic description of the vortex nucleation needs to be modified in a finite trap geometry and the explanation of vortex nucleation requires a detailed analysis of the condensate at its surface or edge (for a two-dimensional geometry). Though the local theory takes different form to analyze the experiments based on different mechanism to rotate the trap, the unifying aspect of these approaches is the role played by surface Bogoliubov excitations. There are many issues related to the nucleation of vortices in BEC that have not been discussed in this article. They include for instance the problem of vortex nucleation in attractive condensate, the dynamics and evolution of the vortex lattice state and the nature of the many-vortex state in a rapidly rotating BEC. All these problems constitute an active domain of research both on experimental and theoretical fronts. Also for the topic discussed, the choice of the references which we have selected for our discussion is not all-inclusive due to the limitation of space. We take this opportunity to apologize for what is left out and to mention that this by no means diminishes their importance. For a more complete account we again refer to the review by Fetter [18] and the references therein.

Acknowledgements

This work primarily grows out of a collaboration with Prof. Eric Akkermans to whom I owe much of my understanding about vortices in BEC. I am very grateful to him for a very careful reading of the manuscript. I am also very thankful to Prof. Assa Auerbach for many discussions on vortex physics and particularly on Bogoliubov excitations. I would also take this opportunity to thank Dr. Subhasis Sinha for many general discussions on rotating condensates. This work is supported by the Israel Council for Higher Education, the Technion, the Israel Academy of Sciences and the fund for promotion of Research at the Technion.

[1] A.J. Leggett, *Physica Fennica* **8**, 125, (1973).

- [2] L. Onsager, *Nuovo Cimento* **6**, Suppl. 2, 249 and 281 (1949).
- [3] R.P. Feynman, Application of Quantum Mechanics to Liquid Helium in *Progress in Low Temperature Physics I*, Edited by C. J. Gorter (North-Holland Publishing Co., Amsterdam, 1955), Chapter 2.
- [4] C. Pethik and H. Smith, *Bose-Einstein Condensation in Dilute gases*, (Cambridge University Press, 2002).
- [5] L. Pitaevskii and S. Stringari, *Bose-Einstein Condensation*, (Oxford Science Publication, 2003).
- [6] F. Dalfovo, S. Giorgini, L. P. Pitaevskii, and S. Stringari, *Rev. Mod. Phys.* **71**, 463 (1999).
- [7] Y. Castin, *Bose-Einstein condensates in atomic gases: simple theoretical results*, in *Coherent atomic matter waves*', Lecture Notes of Les Houches Summer School, edited by R. Kaiser, C. Westbrook, and F. David, EDP Sciences and Springer-Verlag (2001), arXiv cond-mat/0105058.
- [8] M.R.Mathews, B.P. Anderson, P.C. Haljan, D.S. Hall, C. E. Weiman and E. A. Cornell, *Phys. Rev. Lett.* **84** , 2498, (1999).
- [9] P.C. Haljan, I. Coddington, P. Engels and E.A. Cornell , *Phys. Rev. Lett.* **87**, 210403, (2001).
- [10] K. W. Madison, F. Chevy, W. Wohlleben, and J. Dalibard, *Phys. Rev. Lett.* **84**, 806 (2000).
- [11] K. W. Madison, F. Chevy, W. Wohlleben, and J. Dalibard, *J. Mod. Optics* **47**, 2715 (2000).
- [12] F. Chevy, K. W. Madison, and J. Dalibard, *Phys. Rev. Lett.* **85**, 2223 (2000).
- [13] F. Chevy, K. W. Madison, V. Bretin and J. Dalibard: arXiv: cond-mat/0104218.
- [14] K. W. Madison, F. Chevy, V. Bretin and J. Dalibard, *Phys. Rev. Lett.* **86**, 4443 (2001).
- [15] J. R. Abo-Shaeer, C. Raman, J. M. Vogels and W. Ketterle, *Science*, **292**, 476 (2001).
- [16] J. R. Abo-Shaeer, C. Raman and W. Ketterle, *Phys. Rev. Lett.* **88**, 070409 (2002).
- [17] E. Hodby, G. Hechenblaikner, S. A. Hopkins, O. M. Maragò, and C. J. Foot *Phys. Rev. Lett.* **88**, 010405 (2002).
- [18] A. L. Fetter and A. S. Svidzinsky, *J. Phys. Cond. Matt* **13** R135 (2001).
- [19] J. P. Blaizot and G. Ripka, *Quantum Theory of Finite systems*, The MIT Press, Cambridge, Mass. (1985).
- [20] N. N. Bogoliubov, *J. Phys. (USSR)* **11**, 23 (1947).
- [21] A.L. Fetter: *Phys. Rev.* **138** (1965) A709, *Phys. Rev.* **140** (1965) A452, and *Ann. Phys. (N. Y.)* **70** (1972) 67.
- [22] M. Edwards, R. J. Dodd, C.W. Clark and K. Burnett, *J. Res. Natl. Inst. Stand. Technol.* **101**,

553 (1996) and P. A. Ruprecht, M. Edwards, K. Burnett and C.W. Clark, Phys. Rev. A **54**, 4178 (1996).

[23] A. L. Fetter, Phys. Rev. A **53**, 4245 (1996).

[24] R. J. Dodd, K. Burnett, M. Edwards and C. W. Clark, Phys. Rev. A **56**, 587 (1997).

[25] D. S. Rokhsar, Phys. Rev. Lett. **79**, 2164 (1997).

[26] A.L.Fetter and D. Rokshar, Phys. Rev. A **57**, 1191 (1998).

[27] A. Svidzinsky and A. L. Fetter, Phys. Rev. A **58**, 3168 (1998).

[28] T. Isoshima and K. Machida, Phys. Rev. A **59**, 2203 (1999).

[29] T Isoshima and K. Machida, Phys. Rev. A **60**, 3313 (1999).

[30] T. Mizushima, T. Isoshima, and K. Machida, Phys. Rev. A **64**, 043610 (2001); T. Isoshima, Ph.D. Thesis *unpublished*.

[31] A. L. Fetter, J. Low Temp. Phys. **113**, 198 (1998).

[32] T. P. Simula, S. M. M. Virtanen and M. M. Salomaa, Phys. Rev. A **66**, 035601 2002.

[33] E. P. Gross, Nuovo Cimento **20**, 454 (1961).

[34] L. P. Pitaevskii, Zh. Eksp. Teor. Fiz. **40**, 646 (1961) [Sov. Phys. JETP **13**, 451 (1961)].

[35] R. P. Feynman, Phys. Rev. **94**, 262 (1954).

[36] A. Mann, Phys. Rev. A **4**, 750 (1971).

[37] P. Nozières and D. Pines, *The Theory of Quantum Liquids* Volume II (Addition Wesley Pub. Co.,Inc),,1990.

[38] R. J. Donnelly, *Quantized Vortices in Helium II* (Cambridge University Press, Cambridge, U. K., 1991).

[39] V. L. Ginzburg and L. P. Pitaevskii, Zh. Eksp. Teor. Fiz. **34**, 1240 (1958) [Sov. Phys. JETP **7**, 858 (1958)].

[40] G. Baym and C. Pethick, Phys. Rev. Lett. **76**, 6 (1996).

[41] F. Dalfovo and S. Stringari, Phys. Rev. A **53**, 2477 (1996).

[42] F. Dalfovo, L. Piataevskii and S. Stringari, J. Res. Natl. Inst. Stand. Technol. **101**, 537 (1996).

[43] D. A. Butts and D. S. Rokhsar, Nature **397**, 327 (1999).

[44] A. A. Svidzinsky and A. L. Fetter, Phys. Rev. Lett. **84**, 5919 (2000).

[45] M. Linn and A. L. Fetter, Phys. Rev. A **60**, 4910 (1999).

[46] E. Lundh, C. J. Pethick, and H. Smith, Phys. Rev. A **55**, 2126 (1997).

[47] S. Sinha, Phys. Rev. A **55**, 4325 (1997).

- [48] D. Feder *et. al.*, Phys. Rev. Lett. **82**, 4956 (1999).
- [49] S. Stringari, Phys. Rev. Lett. **77**, 2360 (1996).
- [50] F. Zambelli and S. Stringari, Phys. Rev. Lett. **81**, 1754 (1998).
- [51] F. Dalfovo, L. Pitaevskii and S. Stringari, Phys. Rev. A **54** (1996) 4213.
- [52] A. L. Fetter and D. L. Feder, Phys. Rev. A **58**, 3185 (1998).
- [53] U. A. Khawaja, C. J. Pethick and H Smith, Phys. Rev. A **60**, 1507 (1999)
- [54] F. Dalfovo and S. Stringari, Phys. Rev. A **63**, 011601(R) (2000).
- [55] J. R. Anglin, Phys. Rev. Lett. **87**, 240401 (2001).
- [56] L. D. Landau, J. Phys. (U.S.S.R) **5**, 71, (1941).
- [57] E. Akkermans and S. Ghosh, J. Phys. B: At. Mol. Opt. Phys., **37**, S127 (2004); arXiv:cond-mat/0310715.
- [58] A. Recati, F. Zambelli, and S. Stringari, Phys. Rev. Lett. **86**, 377 (2001).
- [59] S. Sinha and Y. Castin, Phys. Rev. Lett. **87**, 190402 (2001)
- [60] M. Kraemer, L. Pitaevskii, S. Stringari and Zambelli, Laser Physics **12**(1), 113 (2002).
- [61] A. L. Fetter and J.D. Walecka, *Quantum Theory of Many Particle Systems*, New York: McGraw-Hill, 1971.
- [62] O. Penrose, Philos. Mag. **42**, 1373 (1951); O. Penrose and L. Onsager, Phys. Rev. **104**, 576.
- [63] Y. Castin and R. Dum, Eur. Phys. J. D **7**, 399 (1999).
- [64] S. Stringari, Phys. Rev. Lett. **82**, 4371 (1999).
- [65] O. Bohigas *et. al.*, Phys. Rep. **51**, 267 (1979); E. Lipparini ad S. Stringari, Phys. Rep. **175**, 103 (1989).
- [66] J.E. Williams and M. J. Holland, Nature **401**, 568 (1999).
- [67] B. P. Anderson, P. C. Haljan, C. E. Weiman and E.C. Cornell, Phys. Rev. Lett. bf 85 2857 (2000).
- [68] A. A. Abrikosov, JETP **32**, 1442 (1957).
- [69] H. Lamb, *Hydrodynamics*, 6th edition (Dover, New York, 1945), pp. 86-88.
- [70] A. A. Svidzinsky and A. L. Fetter, Physica B **284-288**, 21 (2000).
- [71] Y. Castin and R. Dum, Phys. Rev. Lett. **77**, 5315 (1996); V. M. Pérez-García, H. Miinchinel, J. I. Cirac, M. Lewenstein and P. Zoller, Phys. Rev. A **56**, 1424 (1997); E Lundh, C. . Pethick and H. Smith, Phys. Rev. A **58**, 4816 (1998)
- [72] M. Edwards, R. J. Dodd, C. W. Clark, P. A. Ruprecht, and K. Burnett, Phys. Rev. A **51**,

1382 (1995).

- [73] E. Akkermans and R. Narevich, Phil Mag. B **77**, 1097 (1998); E. Akkermans, J. E. Avron, R. Narevich and R. Seiler, Eur. Phys. J. B **1**, 117, (1998)
- [74] R. Narevich, *Ph.D. thesis*, Technion I.I.T, Israel (*unpublished*).
- [75] M. Atiyah, V. Patodi and I. Singer, *Math. Proc. Camb. Phys. Soc.* **77**, 43, (1975).
- [76] M. Guilleumas and R. Graham, Phys. Rev. A, **64**, 033607 (2001)
- [77] B. M. Caradoc-Davies, R. J. Ballagh and K. Burnett, Phys. Rev. Lett. **83**, 895 (1999); D. L. Feder, C. W. Clark and B. I. Schneider, Phys. Rev. A **61**, 011601 (2000)